COMPARATIVE METHANE EMISSION MAPPING IN DELTA AND ADAMAWA STATES VIA SENTINEL 5P OBSERVATIONS FROM 2022-2024

BY

ELIJAH EMMANUEL EDET

LSC2009791

DEPARTMENT OF ENVIRONMENTAL MANAGEMENT AND TOXICOLOGY

FACULTY OF LIFE SCIENCES

UNIVERSITY OF BENIN

BENIN CITY

NOVEMBER 2025.

COMPARATIVE METHANE EMISSION MAPPING IN DELTA AND ADAMAWA STATES VIA SENTINEL 5P OBSERVATIONS FROM 2022-2024

BY

ELIJAH EMMANUEL EDET

LSC2009791

AN UNDERGRADUATE DISSERTATION SUBMITTED TO THE DEPARTMENT OF ENVIRONMENTAL MANAGEMENT AND TOXICOLOGY, FACULTY OF LIFE SCIENCES, UNIVERSITY OF BENIN, BENIN CITY, EDO STATE: IN PARTIAL FULFILLMENT OF THE REQUIREMENTS FOR AWARD OF BACHELOR OF SCIENCE (B.Sc) DEGREE IN ENVIRONMENTAL MANAGEMENT AND TOXICOLOGY,

NOVEMBER 2025

CERTIFICATION

This is to certify that this research titled " Comparative methane emission mapping in Delta and Adamawa states via Sentinel 5P observations from 2022-2024 " was carried out by "Elijah Emmanuel Edet" and presented to the Department of Environmental Management and Toxicology, Faculty of Life Sciences, University of Benin, Benin City; in partial fulfillment of the requirements for the award of Bachelor of Science (B.Sc) in Environmental Management and Toxicology. It was conducted under suitable conditions, was carefully supervised and subsequently approved as having met the requirements for the award of Bachelor of Science degree in Environmental Management and Toxicology.

……..….. ..…..……

PROF. A. A. ENUNEKU Date

Project Supervisor

……..…….. …...……

PROF. (MRS) E. T. AISIEN Date

Head of Department

……..…….. …...……

DR. EGHOMWANRE A.F Date

Project Coordinator

DEDICATION

I would like to dedicate this work to God Almighty for seeing me through every aspect of my life and keeping me to this very moment.

ACKNOWLEDGMENT

I am grateful to God Almighty for his grace and mercy over my life throughout the seminar process. I want to specially thank my Project Supervisor, Prof. A. A. Enuneku for his support and amazing guidance throughout the seminar. Special thanks to the Head of Department Prof. Aisien, my Course Adviser and the project coordinator Dr. Eghomwanre A.F., and the entire lecturers in the department for their investment in my academic development. My appreciation goes to my parents for their care, prayers, financial and emotional support and encouragement. Special gratitude to all my friends especially my comrades Miracle, Osagie, Arize, Seyi, Ojone, Stephanie, Orobosa amongst others that supported me one way or the other. May God richly bless you.

TABLE OF CONTENTS

LIST OF FIGURES

LIST OF TABLES

LIST OF PLATES

ABSTRACT

Methane (CH_4), with warming potential 84 times greater than CO_2 over 20 years, requires urgent mitigation for climate stabilization. This study compared atmospheric methane patterns between Delta and Adamawa States, Nigeria, using 2022–2024 Sentinel-5P TROPOMI satellite data processed through Google Earth Engine. Applying strict quality controls (qa_value ≥ 0.75) and statistical analysis (Mann-Whitney U test, Getis-Ord Gi*), the research revealed distinct emission signatures. Delta State exhibited concentrated industrial emissions, with 96.73% of hotspots at petroleum infrastructure (oil facilities, gas flaring, pipelines). Concentrations increased 1.37% from 1,915.47 to 1,941.72 ppb, showing high spatial heterogeneity (σ = 14.82 ppb) and minimal climate sensitivity. Adamawa State showed diffuse biogenic emissions from livestock (38.84%), waste (17.52%), and wetlands (25.80%), with 0.81% concentration increase (1,925.82 to 1,941.45 ppb), lower variability (σ = 9.85 ppb), but strong climate dependence (ρ = +0.58, $p < 0.001$). Both states showed accelerating trends (Delta: +13.05%/year; Adamawa: +11.38%/year), contradicting Nigeria's 30% reduction pledge by 2030. Results demonstrate that industrial and agricultural sources require distinct strategies: leak detection and infrastructure modernization for petroleum operations versus improved livestock management and waste infrastructure for agricultural systems. This baseline enables future monitoring of mitigation effectiveness.

Keywords: Methane emissions, Sentinel-5P TROPOMI, petroleum industry, livestock agriculture, Nigeria, climate mitigation

1.0 INTRODUCTION

1.1 BACKGROUND INTRODUCTION

Methane (CH_4) is seen as the second most significant anthropogenic greenhouse gas after carbon dioxide (CO_2) and also a principal precursor of tropospheric ozone (Shindell *et al.,* 2012). Aside from playing the role of a greenhouse gas, CH_4 is a secondary atmospheric pollutant that acts as a precursor to the formation of tropospheric ozone consequent upon photochemical oxidation and hence impacts human health, crop yields, and vegetation health. It is also a contributor to Earth's radiative forcing due to its strong absorption in the infrared spectrum band (IPCC, 2023). Methane is a potent greenhouse gas that contributes significantly to global warming, with a warming potential over 80 times that of carbon dioxide in its first 20 years of release (G. Myhre *et al.,* 2013). Despite its short atmospheric lifespan, methane accounts for nearly half a degree Celsius of the modern global temperature rise.

It contributes to global warming after carbon dioxide, accounting for at least one quarter of the present-day warming (Jacob *et al.,* 2022). Accurately quantifying CH_4 emissions from the oil and natural gas (OandG) infrastructure, which is one of the largest sources of anthropogenic CH_4, has been the focus of a large body of research over the past few years (Turner *et al.,* 2019).

Over the past decade, the adoption of low-Earth-orbit satellites to measure and quantify methane (CH_4) emissions has garnered significant attention (Zhu *et al.,* 2025).

Methane is the second most important anthropogenic greenhouse gas in the atmosphere after carbon dioxide (Intergovernmental Panel on Climate Change [IPCC], 2021). CH_4 emissions are related to (i) the production of fossil fuels, e.g. crude oil, natural gas and coal, and can also be released from natural seeps, (ii) microbial processes in wetlands, rice cultivation, livestock,

landfills and termites, and (iii) biomass burning (Saunois *et al.,* 2020). Due to an imbalance between methane sources and sinks, the atmospheric mixing ratio has increased from a pre-industrial value of 722 ppb (IPCC, 2021) to the current global average of approximately 1850 ppb (Lan *et al.,* 2024). As the atmospheric lifetime of methane is relatively short at 9.1 years (IPCC, 2021), a reduction in its emissions would lower the combined radiative forcing from greenhouse gases on a timescale of years and is therefore a relatively efficient option to mitigate climate change.

Methane, a truly influential greenhouse gas, has a vital impact on the chemical composition of Earth's atmosphere and the dynamics of its climate (Schmidt and Shindell, 2003). The rising attention of this substance in the atmosphere has been associated with global warming and large-scale environmental impacts (Kabir *et al*., 2023). Given Nigeria's status as Africa's most populated nation and one of its largest economies, comprehending methane dynamics is vital (Herbst, 1996). This is mainly because of the country's growing industrialization, urbanization, and agricultural expansion. These variables contribute to both natural and manmade sources of methane emissions, ranging from estate operations analogous as cattle tending and rice cultivation to archconservative energy production and waste operation styles (Karakurt *et al*., 2012). Although Nigeria plays a vital part in the indigenous and global methane budget, the country has faced limitations in conducting thorough evaluations of methane emissions due to difficulties in accessing data, achieving high capabilities (Ogbowuokara *et al*., 2023)

Methane (CH4) has a 20-times global warming potential, 85times that of carbon dioxide (CO2) and is an important contributor to decadal climate changes (IPCC, 2021). Mean global methane concentrations have overall climbed for 2020 to 1879 ppb, 2. 6 times that of pre, industrial times, with a recent rate of growth acceleration (1015 ppb yr1 in 2019-2020) of which

the reason is not very clear (NOAA, 2022; Peng et al., 2022; Saunois et al., 2020; Stevenson et al., 2022).

Information on methane emissions is demanded at global, public, and indigenous levels to guide climate action on methane. Current bottom-up inventories are constantly shy of this purpose because of their large misgivings in emigration factors and lack of information on emigration exertion (Saunois *et al*., 2020).

Methane (CH4) is an important greenhouse gas, with a global warming potential 80 times that of carbon dioxide (CO2) on a 20- time timescale and 30 times on a 100- time timescale (Forster *et al*., 2021). In 2020, the atmospheric methane concentration increased to 1889 2ppbv, 262 above pre-industrial levels in 1750, driven primarily by anthropogenic emissions (WMO, 2021). The last decade has seen rapid-fire- fire growth of atmospheric methane (86ppbva 1), after a brief period of stabilisation in the early 2000s (Dlugokencky *et al*., 2011; Fletcher and Schaefer, 2019; Rigby *et al*., 2008; Yin *et al*., 2021; Zhang *et al*., 2021). Rising methane attention, if continued at current rates in the coming decades, may negate the benefits of CO2 emission reduction. That's why reducing methane emissions in the 2020s is essential for the Paris Agreement to be successful (Ganesan *et al.,* 2019; Nisbet *et al.,* 2019).

Anthropogenic methane emissions have caused at least 25 of mortal- convinced global warming (Ocko *et al*., 2018; IPCC, 2021). Methane's atmospheric attention has increased by a factor of 2.5 since the pre-industrial period (Szopa *et al*., 2021), and the rate of increase has accelerated in recent times (NOAA, 2022). Due to its fairly short atmospheric life span and large global warming eventuality (81 times that of CO2 over a time span of 20 years (IPCC, 2021)), methane has an important part in the rate of climate warming (Nisbet *et al*., 2020; Ocko *et al*., 2021; Szopa *et al*., 2021). Reducing global methane emissions is therefore vital to achieve the

pretensions set out in the 2015 Paris Climate Accords (Nisbet *et al*., 2020). Since November 2021, over 125 countries have signed the Global Methane Pledge (European Commission, 2021; CCAC, 2022) and committed to reducing their methane emissions by 30 in 2030 compared to 2020 levels. This could help avoid 0.2 °C of global mean warming by 2050 (CCAC, 2022; UNEP and CCAC, 2021). In order to reduce global methane emissions promptly and effectively during this decade, it is consummated to identify the largest anthropogenic sources of methane and mitigate those. We therefore propose an automated discovery and monitoring system using satellite data with machine learning models to detect methane super-emitters. The dominant anthropogenic methane emission sources are husbandry (beast and rice civilization), oil painting, oil and gas exploitation, waste operation, and coal mining; the precise locales and amounts of emissions are still uncertain (Saunois *et al*., 2020). Large fractions of methane emissions in various sectors could be eased using being technology, with about a quarter of those at no net cost (Nisbet *et al*., 2020; Ocko *et al*., 2021; Lauvaux *et al*., 2022).

Understanding the methane (CH4) global budget coupled with implementing possible mitigation measures is crucial to figuring out viable paths towards the reduction of climate change effects (Saunois *et al*., 2020). Research has shown that urban areas are responsible for about 20% of global anthropogenic CH4 emissions, and these emissions are mainly concentrated in small areas (Hopkins *et al*., 2016; Marcotullio *et al*., 2013). Livestock activities worldwide are responsible for around 32% of the anthropogenic methane emissions, with sub-Saharan Africa becoming the most significant hotspot due to its dependence on pastoral agriculture (FAO, 2023). The livestock sector in Nigeria is a major contributor to national emissions. For instance, the Mubi cattle market in Adamawa State is among the significant sources of emissions due to enteric fermentation and manure management. Despite that, the lack of modern structures emphasizes

the necessity for sophisticated instruments to gauge and lessen the sector's environmental impacts, especially methane emissions.

Methane is the second most important trace gas one of the major contributors to the greenhouse effect which is responsible for approximately 20% of its direct radiation force and its global warming impact is 23 times that of CO2 (Nisbet *et al*., 2019; Niu *et al*., 2019).

The rapidly increasing methane (CH_4) concentration in the atmosphere is a major topic of investigation in modern atmospheric and climate science due to the fact that methane is a powerful short-lived climate pollutant (SLCP). Methane has a radiative forcing power which is about 84 times higher than that of carbon dioxide (CO_2) over 20 years, so cutting it down effectively and promptly is a high-leverage, low-cost way of achieving near-term climate stabilization (Forster *et al*., 2021; IPCC, 2021; Saunois *et al*., 2020). Consequently, pinpointing the exact locations where CH_4 emissions take place and determining their volumes are the very first steps towards drafting, validating, and enforcing effective climate mitigation policies at the national and supranational levels and checking the compliance with international agreements. Worldwide, these emission sources intricately involve both natural ones, such as emissions from large tropical wetlands and geological seeps from deep within the earth, and a multitude of highly concentrated anthropogenic sources. The latter include the huge global oil and gas industry, the spread of intensive agricultural practices, the large-scale accumulation of urban waste in unmanaged landfills, and the occurrence of biomass burning. In areas with high economic stratification and significant geophysical heterogeneity, such as West African sub-region, the problem of accurately identifying and quantifying these different regional fluxes and

figuring out which sector is dominant is a massive and scientifically important methodological challenge.

Satellite-based remote sensing technology has consequentially emerged as an indispensable, objective, and globally consistent mechanism for planetary-scale atmospheric monitoring, providing high-frequency, standardized, and globally comparable data. Specifically, the TROPOspheric Monitoring Instrument (TROPOMI), housed aboard the Sentinel-5 Precursor (S5P) satellite, offers an unprecedented combination of full global daily coverage and high spatial resolution (approximating 5.5 km × 7 km per pixel post-commissioning), rendering it uniquely efficacious for the systematic detection, quantification, and mapping of persistent and episodic CH_4 enhancements at the regional and sub-national levels (European Space Agency, 2024; Hu *et al.,* 2016; Veefkind *et al.,* 2012). This advanced capability provides the necessary empirical means to circumvent the inherent spatial discontinuity, temporal lag, high operational cost, and resource intensity limitations traditionally associated with ground-based monitoring networks. The CH_4 retrieval algorithm employed by TROPOMI leverages measurements in the near-infrared (NIR) and short-wave infrared (SWIR) spectral bands, which confer requisite sensitivity to the total atmospheric column extending down to the planetary surface, making it ideal for detecting near-surface industrial and biogenic sources (Hasekamp *et al.,* 2019; Landgraf *et al.,* 2016; Lorente *et al.,* 2021). The Nigerian Federation, by virtue of its distinct dual economic and ecological profile, is positioned as a major global emitter and thus presents a compelling and representative case study: its CH_4 emissions are driven by two fundamentally distinct economic and ecological regimes—the petrogenic dominance of the southern Niger Delta, characterized by intense hydrocarbon extraction, and the large-scale agrarian and natural biogenic activities characterizing the northern savannah and plateau regions, marked by extensive pastoralism and wetlands. The rigorous comparative assessment of these two

antithetical regimes across the three-year period (2022–2024) forms the core investigative basis for this project, serving to delineate and quantify their respective contributions to the national atmospheric methane load. The study is particularly timely given the recent intensification of global climate targets and the necessity for quantifiable, location-specific emission reduction strategies.

1.2 STATEMENT OF THE PROBLEM

Despite the fact of Nigeria's substantial and globally recognized contribution to the global methane burden (Saunois *et al.,* 2020), there persists a critical and consequential lacuna in the spatially explicit, contemporary (2022–2024), and quantitative comparative analysis of its principal regional emission drivers. This significant gap is a function of reliance on generalized Tier I national inventory methodologies, which do not account for sub-national source intensity. The comprehensive research problem, therefore, is threefold, demanding the application of high-resolution satellite data and advanced statistical methods to address specific regional complexities that demonstrably evade traditional reporting methods.

First, within Delta State, which constitutes the economic and geographic heart of the Nigerian petroleum industry and is defined by the vast, complex, and hydrologically active Niger Delta ecosystem, the paramount challenge resides in the accurate and definitive disaggregation of high-magnitude, intermittent, and often fugitive petrogenic emissions from the persistent, lower-flux biogenic background. The petrogenic emissions (emanating from routine gas flaring, unauthorized venting, and pervasive leaks across a vast, aging pipeline and processing network) are characterized by extreme spatial heterogeneity and periodicity, presenting as intense, transient plumes (Afinotan, 2022; Omojola, 2014; Ukhurebor *et al.,* 2024). This signal must be statistically separated from the relatively constant, large-area flux produced by the extensive coastal, tidal, and riverine wetland systems and mangrove forests. Existing national emission

inventories frequently rely upon generalized, aggregated activity data (e.g., total crude production or estimated flare volumes), which systematically fail to capture the high-frequency temporal and spatial variability characteristic of industrial point-source emission plumes. This reliance introduces significant systemic uncertainty in source attribution and fundamentally hinders the implementation of targeted regulatory enforcement at the local level.

Second, and in direct environmental contrast, Adamawa State is overwhelmingly dominated by agricultural and natural biogenic sources, a condition reflective of its location within the Guinea and Sudan savannah belts. The principal sources are associated with extensive pastoralism, intensive livestock management, and localized rice cultivation, which contribute substantial volumes of methane through enteric fermentation and subsequent manure management practices (Johnson and Johnson, 1995; Knapp *et al.,* 2014). The precise magnitude, spatial density, and temporal seasonality of these agrarian-driven fluxes necessitate objective quantification against the distinct geophysical background of a semi-arid climate, low surface albedo, and the elevated, complex topography of the Adamawa Plateau. The potential for these topographical and surface property effects to systematically influence CH_4 retrieval accuracy further complicates the analysis without the application of rigorous, scientifically validated quality control (QC) filtering protocols. A key uncertainty lies in determining the relative contribution of extensive pastoralism versus natural savannah wetlands to the total CH_4 column.

The overarching problem is the prevailing lack of contemporary, high-resolution data (2022–2024) and the necessary analytical framework that prohibits the statistically robust comparison of the median methane burden and specific emission clustering patterns between these two ecologically and industrially antithetical administrative regions. Consequently, the core research problem is defined by the absence of a methodologically rigorous, quantitative, and comparative assessment—executed utilizing advanced geospatial processing techniques within the scalable

environment of the Google Earth Engine (Gorelick *et al.,* 2017)—to objectively determine whether a statistically significant difference exists in the atmospheric methane concentration profiles of Delta and Adamawa States, and to definitively spatially attribute the causative anthropogenic and biogenic sources of any detected disparity to support evidence-based policy formulation.

1.3 AIMS AND OBJECTIVES

Aim

The **Aim** of this project is to execute a rigorous quantitative comparative analysis of atmospheric methane emission patterns across Delta and Adamawa States, utilizing the full temporal archive of Sentinel-5P/TROPOMI observations spanning the three years from January 2022 to December 2024, thereby providing a contemporary assessment of regional emission heterogeneity.

Objectives:

1. To process Sentinel-5P methane data for both states using strict quality control filters (qa_value ≥ 0.7) that remove errors from clouds, aerosols, and surface reflectance, ensuring reliable data for analysis.
2. The study uses the Mann-Whitney U test to compare the median methane levels (XCH_4) from Delta and Adamawa States, accounting for non-normal data distribution, to determine if a significant difference exists between them.
3. To use the Getis-Ord Gi statistic to spatially map and confirm persistent areas of abnormally high methane concentration (hotspots) in Delta and Adamawa States with statistical certainty.

4. Calculate the annual rate of emission change in each state (2022–2024) using time-series analysis to determine if methane levels are increasing, decreasing, or stable.

5. **Identify the specific economic activities or natural processes** causing the hotspots by comparing their locations to land-use maps and industrial records.

1.4 Justification

The present investigation possesses profound and multifaceted scientific, policy, and geographical justification, significantly exceeding a mere academic exercise and moving toward applied environmental intelligence.

Scientifically, the research contributes substantively to the methodological validation and technical refinement of high-resolution atmospheric sensing by TROPOMI within challenging tropical and West African environments. The rigorous application of enhanced quality control and cloud masking protocols, coupled with the computational scalability and massive data access facilitated by the Google Earth Engine, provides a robust and replicable framework for sub-national atmospheric monitoring across the African continent (Gorelick *et al.,* 2017). Furthermore, by comparing a wetland/industrial setting (Delta) with a savannah/agricultural setting (Adamawa), the study provides critical empirical evidence on the differential behavior, spatial clustering, and temporal dynamics of methane emissions under two distinctly different regional climatic and socio-economic contexts within a single nation-state. The resulting CH_4 maps and time series are essential for the calibration and validation of regional climate and atmospheric transport models, which are often poorly constrained by local data.

The **Policy Justification** is deemed paramount in the contemporary climate discourse and national development planning. By objectively quantifying the differential in median CH_4

concentration and precisely localizing emission hotspots via the statistically validated Getis-Ord Gi statistic, the research generates specific, actionable, and geographically explicit intelligence necessary for targeted sub-national mitigation efforts. The capacity to rigorously distinguish the primary driver (industrial vs. agricultural) allows regulatory bodies to efficiently allocate finite monitoring resources and implement specific, effective policy instruments—such as addressing the enforcement of flare-out regulations, improving leak detection and repair (LDAR) within Delta's oil and gas sector (Afinotan, 2022; Omojola, 2014; Osuji and Avwiri, 2005), or subsidizing improved livestock enteric fermentation reduction and manure processing techniques in Adamawa (Hristov *et al.,* 2015; Knapp *et al.,* 2014). The derived, statistically robust data facilitate the establishment of a verifiable, evidence-based baseline for Nigeria's National Determined Contributions (NDC) toward the Global Methane Pledge (IPCC, 2021; Saunois *et al.,* 2020), enhance the nation's capacity for emission reporting transparency, and strengthen its accountability within other international climate change mitigation frameworks. By identifying the relative magnitude of emissions, policy can shift from generalized national mandates to localized, sector-specific interventions.

Geographically and Socio-Economically, this comparative framework establishes a crucial regional baseline for accurate emission inventory generation, moving definitively beyond generalized national estimates, which often mask localized severity. It provides a contemporary CH_4 data record for 2022–2024, enabling future researchers and policymakers to objectively assess the success or failure of regulatory interventions and environmental policies over time using a standardized metric. By linking specific economic activities (oil and gas infrastructure, concentrated cattle routes, and agricultural practices) to demonstrated environmental risk, the project increases the confidence in the derived source attribution results and their ultimate utility for environmental governance, resource allocation, and regional development planning. The

rigorous, non-parametric statistical approach ensures that the findings are scientifically defensible, thereby bolstering their credibility in high-stakes policy discussions regarding climate change and public health. This localized information is vital for addressing environmental justice issues related to proximity to pollution sources.

2.0: LITERATURE REVIEW

2.1 METHANE IN THE CLIMATE SYSTEM AND ATMOSPHERIC CHEMISTRY

Methane (CH_4) is ascertained to be not merely the second most salient anthropogenic greenhouse gas but also a material precursor for the formation of tropospheric ozone (O_3), which is recognized as a detrimental air contaminant and a potent climate forcing agent. The demonstrably high radiative efficiency inherent in the CH_4 molecule dictates that thermal retention is affected far more substantially than is the case with carbon dioxide (CO_2) on a per-molecule basis, thereby conferring an immediate and intense warming impact. Over a centennial timescale, CH_4 exhibits a Global Warming Potential (GWP) conservatively situated between approximately 28 and 34, which underscores its pronounced potency (Myhre *et al.,* 2013). More significantly, across the critical two-decade temporal horizon (GWP_{20}), its radiative forcing capacity ascends to approximately 86 times that of CO_2 (Forster *et al.,* 2021; IPCC, 2021). This curtailed atmospheric tenure, juxtaposed with the elevated GWP, renders CH_4 mitigation the single most efficacious "fast lever" available for the deceleration of the extant rate of global temperature escalation, thus furnishing a crucial temporal buffer for the resolution of the protracted challenge posed by full energy system decarbonization.

Direct and Indirect Climate Forcing: The CH_4 influence upon the climate system is characterized by a dual mechanism. Directly, the substance facilitates the absorption of outgoing longwave radiation, precipitating the thermal augmentation of the troposphere. Indirectly, its

oxidative pathway within the stratosphere constitutes a source of stratospheric water vapor, itself a powerful greenhouse gas that contributes materially to the genesis of polar stratospheric clouds. Furthermore, its principal atmospheric sink, the reaction with the hydroxyl radical (OH), exerts control over the OH concentration (Levy, 1971; Stevenson *et al.,* 2020). This constitutes a fundamental atmospheric self-regulating mechanism; as CH_4 concentrations accrue, available OH is systematically consumed. The concomitant diminution of the OH reservoir thereby inadvertently impedes the natural cleansing capacity of the atmosphere, resulting in the extension of the effective lifetime not solely of CH_4 itself but also of other climate-active gases, such as hydrofluorocarbons (HFCs), thereby establishing a positive, self-amplifying feedback mechanism in relation to atmospheric warming. This chemical complexity necessitates precise measurement and rigorous attribution of source origins for the effective prediction and control of future warming trajectories.

The atmospheric residency period of CH_4 is relatively brief (estimated at 9–12 years), the duration of which is primarily constrained by reaction with the hydroxyl radical (OH), conventionally designated as the "detergent of the atmosphere" (Levy, 1971; Prather *et al.,* 2012; Stevenson *et al.,* 2020). Notwithstanding this, as CH_4 concentrations escalate, the available OH is consumed, with the potential consequence of diminishing the global OH reservoir. This inherent self-limiting feedback loop potentially extends the CH_4's lifetime, presenting a significant impediment to the accurate construction of future climate projections. Global CH_4 sources are systematically compartmentalized into natural contributions (e.g., wetlands, geological seeps) and anthropogenic contributions, which comprise the fossil fuel production sector, agricultural practices (enteric fermentation and manure management), and municipal waste processing. Anthropogenic sources presently account for an approximate 60% share of the

aggregate global CH_4 budget and are the causal factor driving the continuous augmentation in atmospheric concentrations observed subsequent to the year 2007 (Saunois *et al.,* 2020).

2.1.1 REMOTE SENSING OF CH_4 UTILIZING TROPOMI

Satellite remote sensing represents the sole effective methodology for the provision of independent, high-frequency, and global surveillance of CH_4 emissions at scales pertinent to national and regional policy frameworks. The Sentinel-5 Precursor (S5P) satellite, housing the TROPOspheric Monitoring Instrument (TROPOMI), which commenced operation in 2017, has fundamentally redefined this monitoring capability (European Space Agency, 2024; Veefkind *et al.,* 2012). The instrument facilitates the measurement of the column-averaged dry air mole fraction of methane (XCH_4), quantified in parts per billion (ppb), with an empirical cadence of daily global coverage. The instrument features an expansive 2600 km swath width, achieving a spatial resolution of approximately 5.5 × 7 km^2 (subsequent to August 2019), which is of sufficient granularity to permit the detection and precise localization of enhancements originating from both substantial, clustered point sources and extensively diffused area sources (Hu *et al.,* 2016; Veefkind *et al.,* 2012).

• **Measurement Principle and Optimal Wavelength:** TROPOMI operates as a nadir-viewing spectrometer, employing the sun-glint technique over both oceanic and terrestrial surfaces. The sun-glint phenomenon, wherein the instrument registers the specular reflection of incident solar radiation, significantly amplifies the signal-to-noise ratio and, consequently, the measurement sensitivity. Retrieval is executed through the quantification of the absorption of reflected sunlight within the Short-Wave Infrared (SWIR) spectral range (≈ 2300 nm) (Hasekamp *et al.,* 2019; Hu *et al.,* 2016; Landgraf *et al.,* 2016). This spectral window, specifically designated as the SWIR-3 band, is optimal because CH_4 exhibits strong, isolated absorption lines therein, minimizing

spectral interference attributable to water vapor and ozone. Crucially, the radiation path within this band penetrates deeply into the troposphere, rendering the measurement acutely sensitive to CH_4 enhancements proximate to the planetary surface, whence anthropogenic emissions principally originate.

• **Ancillary Correction, Retrieval Challenges, and Averaging Kernel:** The accurate retrieval of XCH_4 is inherently complex, particularly within tropical and arid geographic domains, such as Nigeria, which are frequently subject to high cloud obscuration and substantial seasonal loads of atmospheric aerosols (e.g., particulate matter originating from the Saharan desert). For the precise correction of the total atmospheric mass along the observed light path—a necessary prerequisite for the calculation of the dry air mole fraction—the TROPOMI algorithm concurrently measures the oxygen A-band (≈ 760 nm) (Hasekamp *et al.,* 2019; Landgraf *et al.,* 2016). The total column pressure thus derived from the O_2 A-band is subsequently employed for the calculation of the Air Mass Factor (AMF), which serves to correctly normalize the measured CH_4 absorption to account for variations in viewing geometry and altitude. Effective data utilization mandates the strict adherence to Quality Assurance (QA) values (typically stipulated as QA > 0.5 or QA > 0.8) to systematically filter out observations contaminated by aerosols or clouds, thereby mitigating the presence of retrieval artifacts (European Space Agency, 2024; Lorente *et al.,* 2021). A critical data output is the Averaging Kernel (AK), the integration of which into the analysis is mandatory (Hasekamp *et al.,* 2019; Lorente *et al.,* 2021). The AK matrix provides the quantitative expression of the altitude-dependent sensitivity inherent in the satellite's measurement apparatus. For the precise estimation of flux from surface sources (such as gas flares), it is imperative that observations wherein the AK profile demonstrates high sensitivity within the Planetary Boundary Layer (PBL) be selected, thus preventing the systematic underestimation of surface-level CH_4 enhancements.

2.2 METHODS FOR SOURCE ATTRIBUTION AND QUANTIFICATION

The transition from a satellite-measured concentration (quantified in parts per billion) to an estimated emission flux (mass per unit time) necessitates the application of specialized methodologies, a process of paramount importance for the comparative nature of this study.

1. Enhancement Mapping (Hotspot Analysis) and Background Subtraction: This foundational methodology, which is central to the present comparative investigation, involves the calculation of the local concentration anomaly, alternatively termed the enhancement (XCH_4) (Liu *et al.,* 2021).

$\Delta XCH_4 = XCH_{4,local} - XCH_{4,background}$

The judicious selection of the XCH_4, background value is critical for the effective isolation of the local emission signal. For regional studies, two primary strategies are commonly implemented: (a) The Upwind/Clean-Sector Method, where the background is rigorously defined by the mean concentration measured in an adjacent geographical area confirmed to be free of known emissions and situated meteorologically upwind, and (b) The Percentile Method (e.g., the 10th or 20th percentile of XCH_4 within a circumscribing buffer zone of substantial dimension around the target area). The percentile method is generally favored due to its robust nature against fluctuations in wind patterns and its reduced susceptibility to contamination originating from distant sources. High-resolution TROPOMI data are subsequently utilized for the visual and statistical identification of these enhancements (Liu *et al.,* 2021; Schneising *et al.,* 2019). Localized plumes characterized by steep concentration gradients and elevated peak values constitute the definitive signature of industrial point sources (e.g., hydrocarbon facilities), whereas wider, sustained geographic areas exhibiting lower but persistent concentration levels are characteristic of diffused biogenic area sources (e.g., enteric fermentation zones, extensive

landfills). Subsequent analysis necessitates the spatial binning of the retrieved data onto a regularized grid (0.05° × 0.05° or an equivalent resolution) to harmonize the observational spatial footprint and facilitate accurate comparative analysis across disparate observation periods (Schneising *et al.,* 2023).

2. Emission Quantification (Mass Balance and Modeling): While enhancement mapping is utilized for the identification and characterization of the emission signature, the determination of an accurate flux estimates mandates the integration of meteorological data.

- **Integrated Mass Enhancement (IME) / Mass Balance:** This technique constitutes a robust, semi-quantitative method frequently applied to plumes that are clearly defined and originate from point sources. Its basis lies in the principle of mass conservation, which stipulates that the flux traversing a downwind cross-section of an emission plume must necessarily equate to the source emission rate. The technique entails the integration of the total CH_4 mass contained within the clearly delineated plume area situated downwind of the source. This aggregate mass is then conjoined with concurrent reanalysis wind speed and direction data (e.g., derived from the ECMWF ERA5 global atmospheric reanalysis) (Hersbach *et al.,* 2020). Specifically, the wind velocity component orthogonal to the plume axis is employed to calculate the mass flux traversing the plume's cross-sectional boundary, thereby providing an instantaneous emission rate expressed in kg/s or tonnes/hour. The operational limitation of this method resides in its strict requirement for stable, linear wind conditions and a clear, non-overlapping plume morphology. Furthermore, its typical reliance on manual delineation of the plume boundary introduces an element of subjectivity into the calculation.

o **Gaussian Plume Modeling and Inverse Modeling:** For sources characterized by complexity or regional extent, the utilization of advanced atmospheric dispersion theories becomes

indispensable (Liu *et al.,* 2021). Gaussian Plume Models mathematically approximate the observed XCH_4 enhancement morphology by fitting it to parameterized atmospheric variables (such as planetary boundary layer height, atmospheric stability classes, and effective stack height), permitting robust, albeit simplified, estimations of the source strength for isolated singular sources. For regional, diffused biogenic sources (e.g., waste disposal sites or entire agricultural sectors), complex Lagrangian Particle Dispersion Models (e.g., FLEXPART or WRF-Chem) or high-resolution chemical transport models represent the most definitive standard. These models function 'inversely'—they propagate known background concentrations through high-resolution meteorological fields to determine the spatial and temporal source flux distribution that provides the optimal explanation for the aggregate observed satellite XCH_4 concentration field across the entire domain. Although computationally intensive, these methodologies furnish the most accurate representation of fluxes emanating from spatially distributed area sources.

2.3 METHANE EMISSION PROFILE OF NIGERIA

2.3.1 OIL AND GAS EMISSIONS (THE NIGER DELTA)

The Niger Delta, encompassing jurisdictions such as Delta State, constitutes a global nexus for emissions specifically related to fossil fuel exploitation. The regional emission profile is overwhelmingly dominated by anthropogenic thermogenic sources. The extant Nigerian oil and gas infrastructure, substantial portions of which were installed between the 1960s and 1980s, exhibits considerable age and is afflicted by decades of systematic deferred maintenance, contributing to persistent and, on occasion, catastrophic leakage incidents (Obanijesu *et al.,* 2009; Omojola, 2014; Osuji and Avwiri, 2005).

• **Source Mechanisms and Policy Ineffectiveness:** The two primary emission sources are identified as gas flaring (the purposeful combustion of associated natural gas) and fugitive/venting emissions. Notwithstanding the promulgation of the Nigerian Gas Flare Regulation of 2018, which formally prohibits routine flaring and establishes a framework for gas commercialization, substantial volumes of gas, measured in billions of cubic meters, continue to be flared annually (Afinotan, 2022; American Association for the Advancement of Science, 2011; Omojola, 2014; Ukhurebor *et al.,* 2024). This persistence is directly attributable to the inadequacy of infrastructure designated for gas capture, processing, and transportation (the lack of gas off-takers), thereby rendering flaring the path of least economic resistance for operators. Flaring releases not only CO_2 but also uncombusted CH_4 due to intrinsic incomplete combustion efficiency, particularly during operational phases characterized by instability or high wind velocities. Fugitive emissions—leakages originating from degraded seals, corroded conduits, compression facilities, and storage vessels—are frequently the genesis of the high-magnitude, transient phenomena termed Super-Emitters (Balasus *et al.,* 2023; Liu *et al.,* 2021). TROPOMI has demonstrated a high degree of efficacy in precisely locating these intense, spatially bounded events. This distinct emission profile is therefore characterized by persistence (stemming from routine flaring/venting), high magnitude (derived from super-emitters, with fluxes occasionally exceeding 50 tonnes/hour), and a spatially localized signature, which is frequently co-located with known hydrocarbon production facilities and flow stations. The resulting statistical signature is expected to exhibit elevated peak values but low spatial variance (σ) upon aggregation, as the emission signal is highly concentrated into discrete plumes.

2.3.2 AGRICULTURE AND WASTE EMISSIONS (NORTHERN NIGERIA)

The North East region, as exemplified by Adamawa State, presents a contrasting CH_4 challenge fundamentally dominated by biogenic sources—methane synthesized by microbial action.

• **Livestock, Land Use, and Enteric Fermentation:** The region sustains significant populations of livestock, primarily Zebu cattle, which are indispensable to the socio-economic framework of the area and central to the practice of nomadic pastoralism. The substantial volume of enteric fermentation (digestive processes intrinsic to ruminants) results in massive, yet highly diffused, CH_4 emissions distributed across extensive grazing areas and migratory corridors (Johnson and Johnson, 1995; Knapp *et al.,* 2014). Furthermore, alterations in land-use practices, including the conversion of traditional grazing lands to cultivated areas, may inadvertently foster localized wetland-like conditions that exacerbate natural emissions. The emission intensity per unit area is lower than that associated with a gas flare, but the cumulative effect across the region is substantial due to the vast geographical extent of the activity.

• **Waste Management, Methanogenesis, and Environmental Sensitivity:** The rapid acceleration of urbanisation and the inadequacy of current municipal solid waste (MSW) management practices are factors escalating the CH_4 contribution attributable to waste. Landfills situated within major northern urban centres are typically maintained as open dumps where organic matter undergoes anaerobic decomposition facilitated by methanogenic archaea (Saunois *et al.,* 2020). This biological process is intrinsically sensitive to environmental parameters: optimal CH_4 generation is favoured by elevated ambient temperatures and the presence of adequate, though not surplus, moisture. Consequently, the emissions profile emanating from these sources is inherently diffused across urban agglomerations and characterized by a pronounced seasonal correlation. Higher CH_4 flux rates are typically registered during the transition between the wet and dry seasons, a period when organic matter possesses adequate moisture content and temperatures are sufficiently high to accelerate decomposition kinetics. The

statistical signature is therefore anticipated to be low in magnitude relative to the Delta, but high in spatial variance (σ), which accurately reflects its wide, persistent geographical footprint.

• **Pyrogenic Interference and Data Deconvolution:** The arid climate and agricultural practices endemic to the region also introduce seasonal complexities originating from pyrogenic sources (biomass combustion related to agricultural clearing or naturally occurring wildfires). During the dry season (Harmattan), these combustion events release substantial, short-lived pulses of CH_4 concomitant with carbon monoxide (CO), which serves as a crucial atmospheric tracer for combustion (Schneising *et al.,* 2019). The process of deconvolving the biogenic (enteric/waste) signal from this pyrogenic signal within TROPOMI data streams is acutely challenging, necessitating the deployment of the co-retrieved CO product for the purposes of temporal filtering and definitive source separation.

2.4 GAP ANALYSIS

While TROPOMI data have been successfully utilized for the characterization of both industrial emissions (predominantly within the Niger Delta) and biogenic/waste emissions (across various global regions), a critical deficiency persists: the absence of a direct, contemporaneous, and rigorous comparative analysis conducted between these two distinct and economically vital sectors within a singular national context (Nigeria). Previous scholarly inquiries have systematically analyzed these regions in analytical isolation, thereby precluding the derivation of integrated, prioritized policy recommendations. For example, studies exclusively centered on the Delta have resulted in national policy frameworks unduly skewed toward industrial regulation, concurrently neglecting the accumulating, diffuse risk present in the North.

This research uniquely addresses this analytical deficiency by:

1. Ensuring Methodological Consistency and Data Harmonization: Applying a singular, consistent data preprocessing protocol, Quality Assurance (QA) filtering, and a uniform background subtraction methodology (e.g., the 10th percentile method) to both the fossil fuel-dominated Niger Delta and the agriculture/waste-dominated North East (Liu *et al.,* 2021). This methodological uniformity ensures that the resultant emission signatures are genuinely comparable and demonstrably free from inherent methodological bias. Furthermore, the mandatory application of the Averaging Kernel (AK) correction ensures that both surface-level point sources and column-integrated area sources are accurately represented within the final XCH_4 enhancement maps (Hasekamp *et al.,* 2019; Lorente *et al.,* 2021).

2. Quantifying Signature Differentiation through Variance: Providing a robust statistical comparison of the resultant atmospheric signatures. This objective is attained through the rigorous contrasting of the mean magnitude, temporal persistence, and, crucially, the Spatial Variability (σ) of Delta's high-magnitude plumes (anticipated to exhibit low σ) with Adamawa's wide, persistent enhancements (anticipated to exhibit high σ). This analytical step elevates the findings beyond mere qualitative visual observation to quantifiable, statistical evidence necessary for compliance with Tier 3 inventory reporting standards.

3. Policy Segmentation as a Core Output: Utilising the 2022–2024 observational epoch, which encapsulates post-pandemic industrial activity and aligns precisely with the planning horizon established for national climate pledges. The capacity to definitively differentiate the "high-peak, narrow-base" industrial signature from the "low-peak, broad-base" biogenic signature constitutes the necessary prerequisite for the development of regionally tailored and scientifically defensible mitigation interventions—an essential prerequisite for advancing Nigeria's climate governance apparatus. The resultant policy framework shall be systematically segmented: industrial policy shall be centered upon LDAR (Leak Detection and Repair) and infrastructure modernization

(Afinotan, 2022; Omojola, 2014), while biogenic policy shall be focused upon MSW diversion, landfill gas capture, and enhanced livestock management protocols (Hristov *et al.,* 2015; Knapp *et al.,* 2014). Spatial analysis utilizing Google Earth Engine facilitates the integration of land cover data with emission signatures, thereby enabling precise source attribution and the development of targeted intervention strategies for each emission category (Buchhorn *et al.,* 2020), (Gorelick *et al.,* 2017).

3.0 METHODOLOGY

3.1 STUDY AREAS

This investigation is formally predicated upon a methodical comparative analysis, the scope of which encompasses two geographically and economically disparate regions within the Federal Republic of Nigeria. These designated regions function as statistically robust proxies for the nation's two dominant, and fundamentally antithetical, methane (CH_4) source typologies. This systematic selection ensures that the derived empirical results and subsequent policy prescriptions are capable of direct segmentation and possess verified national relevance.

3.1.1 INDUSTRIAL POINT SOURCE AREA: DELTA STATE, NIGER DELTA (SOUTHERN NIGERIA)

• Context and Significance: Delta State, which is situated within the low-lying, highly humid coastal ecosystem of the Niger Delta, is globally recognized as the operative nucleus of Nigeria's expansive petroleum extraction and processing complex. The region is characterized by a high spatial density of critical energy infrastructure, including a multitude of crude oil flow stations, major refinery apparatus, expansive gas processing installations, and an intricate, frequently decades-old conduit network of high-pressure pipelines. The confluence of the specific

geological structure and the operational environment render this domain highly susceptible to both planned emissions and accidental fugitive releases.

• Emission Profile and Physical Signature: Emissions originating from this designated area are overwhelmingly thermogenic (derived from fossil hydrocarbons) and are statistically characterized by an elevated spatial concentration coupled with a high temporal magnitude. These emissions are the direct consequence of sustained industrial activities, specifically comprising chronic gas flaring operations (the prescribed combustion of associated gas), intentional venting practices (the direct atmospheric release of uncombusted gas), and frequent occurrences of high-flux fugitive leaks from aging apparatus. These source mechanisms generate sharp, spatially and temporally ephemeral plumes that exhibit steep concentration gradients—often generically termed "super-emitter events" (Balasus *et al.,* 2023; Liu *et al.,* 2021)—which remain spatially localized yet contribute disproportionately to the aggregate regional CH_4 budget. The analytical design is specifically calibrated to facilitate the capture and characterization of the statistical signature inherent to this 'spiky' emission typology.

3.1.2 BIOGENIC/AGRICULTURAL SOURCE AREA: ADAMAWA STATE, NORTH EAST (NORTHERN NIGERIA)

• Context and Significance: Adamawa State is geographically situated within the arid and semi-arid savanna zone, positioned remotely from major hydrocarbon production complexes. The state functions as a critical nexus for Nigeria's agricultural sector, sustaining immense populations of livestock, notably the resilient Zebu cattle breeds, and serving as a principal corridor for seasonal nomadic pastoralism. Furthermore, the rapidly expanding urban agglomerations within the state necessitate the deployment of large, non-engineered municipal solid waste (MSW) repositories.

• Emission Profile and Physical Signature: Emissions derived from this proxy region are fundamentally biogenic (microbially synthesized) and are characterized by a wide diffused geographical dispersion and persistent, yet lower-magnitude, concentration levels. The primary causal sources are enteric fermentation intrinsic to ruminant digestive systems (Johnson and Johnson, 1995; Knapp *et al.,* 2014) and methanogenesis (anaerobic decomposition) occurring within the aforementioned waste disposal sites. These processes culminate in the generation of a broad, temporally stable regional CH_4 atmospheric enhancement. Crucially, the kinetic rates of methanogenesis are demonstrably environmentally sensitive, exhibiting a statistically significant dependency upon seasonal fluctuations in ambient temperature and soil moisture/precipitation levels. The analytical objective is rigorously structured to affect the successful differentiation of this spatially uniform, climate-driven 'broad-base' signature from the high-magnitude industrial concentration spikes observed within the Delta State domain.

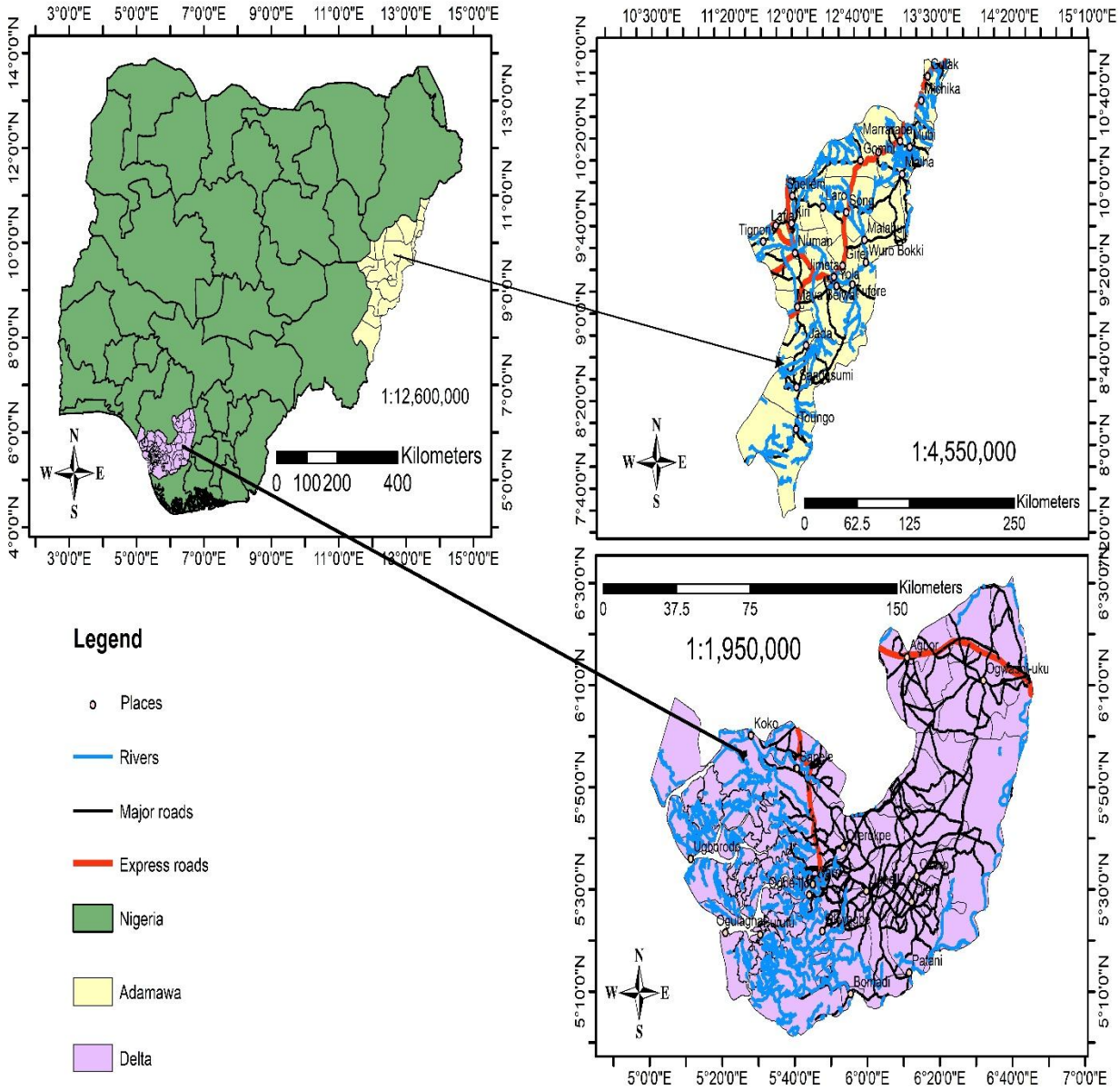

Figure 3.1 study area showing (a) A data frame of a Nigerian map showing DELTA AND ADAMAWA STATES. (b) Map depicting ADAMAWA LGA (c) Map depicting DELTA LGA

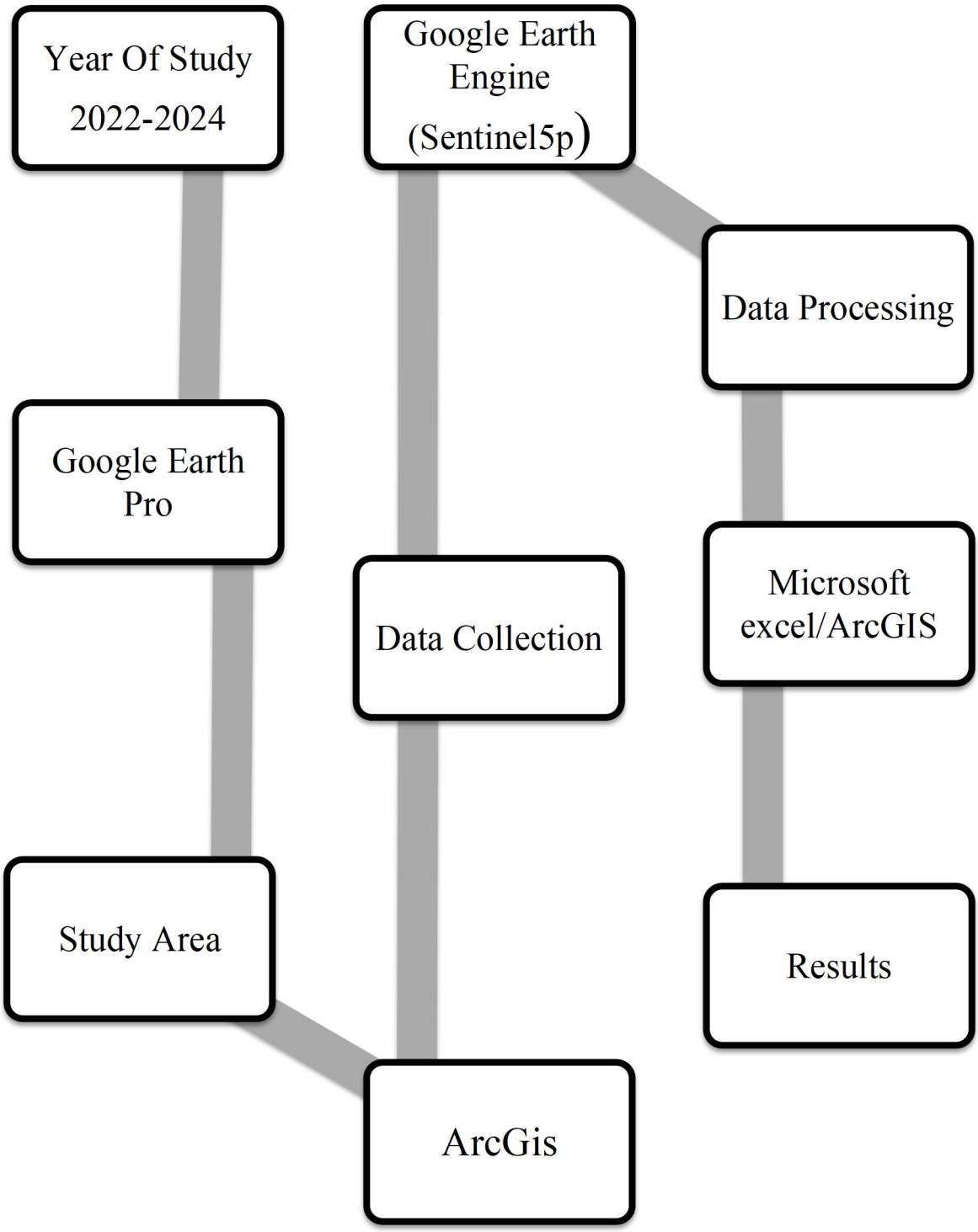

Fig. 3.2 Illustration of the research designs

3.2 ACQUISITION OF DATA AND ANCILLARY METEOROLOGICAL VARIABLES

3.2.1 PRIMARY DATA: TROPOMI XCH_4 AND OBSERVATIONAL STRATEGY

The methodological cornerstone of the present study resides in the utilization of the TROPOspheric Monitoring Instrument (TROPOMI) L2 product (European Space Agency, 2024; Hu *et al.,* 2016), which is efficiently accessed through the expansive and expertly managed Google Earth Engine (GEE) geospatial data catalogue (Gorelick *et al.,* 2017).

• Data Product Specification: The dataset specifically employed constitutes the Sentinel-5 Precursor/TROPOMI L2 Tropospheric Column-Averaged Dry Air Mole Fraction of Methane (XCH_4), the concentration of which is formally quantified in parts per billion (ppb).

• Timeframe Justification: The analysis leverages a comprehensive 36-month observational epoch, commencing precisely on January 1, 2022, and concluding on December 31, 2024. This recent three-year window was strategically selected to furnish a demonstrably large sample size requisite for robust statistical inference, while simultaneously centring the analysis on current, post-pandemic industrial operational activity and contemporary demographic and agricultural trends. The selected duration provided the requisite temporal depth for the capture of seasonal (climate-driven) fluctuations within the North and operational variations within the South.

• Temporal Sampling: TROPOMI maintains a sun-synchronous orbital track, resulting in a consistent local time of observation near 13:30 (1:30 PM) local time on a diurnal basis (European Space Agency, 2024; Veefkind *et al.,* 2012). This specific observation time is deemed optimal due to its general concordance with the period of maximum Planetary Boundary Layer (PBL) height. A deeper, well-mixed PBL provides the most advantageous atmospheric conditions for remote satellite detection, as surface emissions are efficiently lofted and

horizontally distributed throughout the boundary layer, thereby maximizing the sensor's probability of detection and minimizing retrieval uncertainty attributable to shallow or collapsed boundary layers.

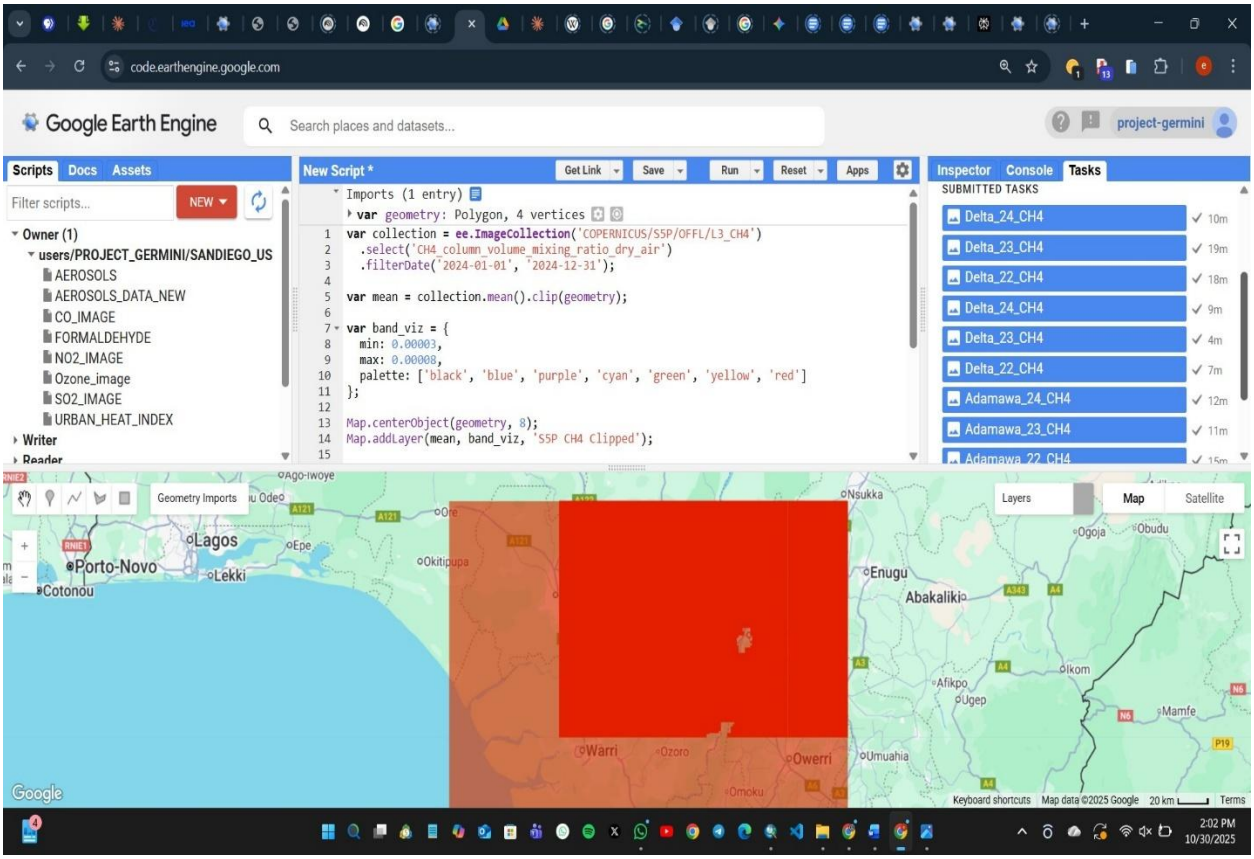

Plate 3.1: Google Earth Engine showing the source JavaScript, successful extractions and a marked study area.

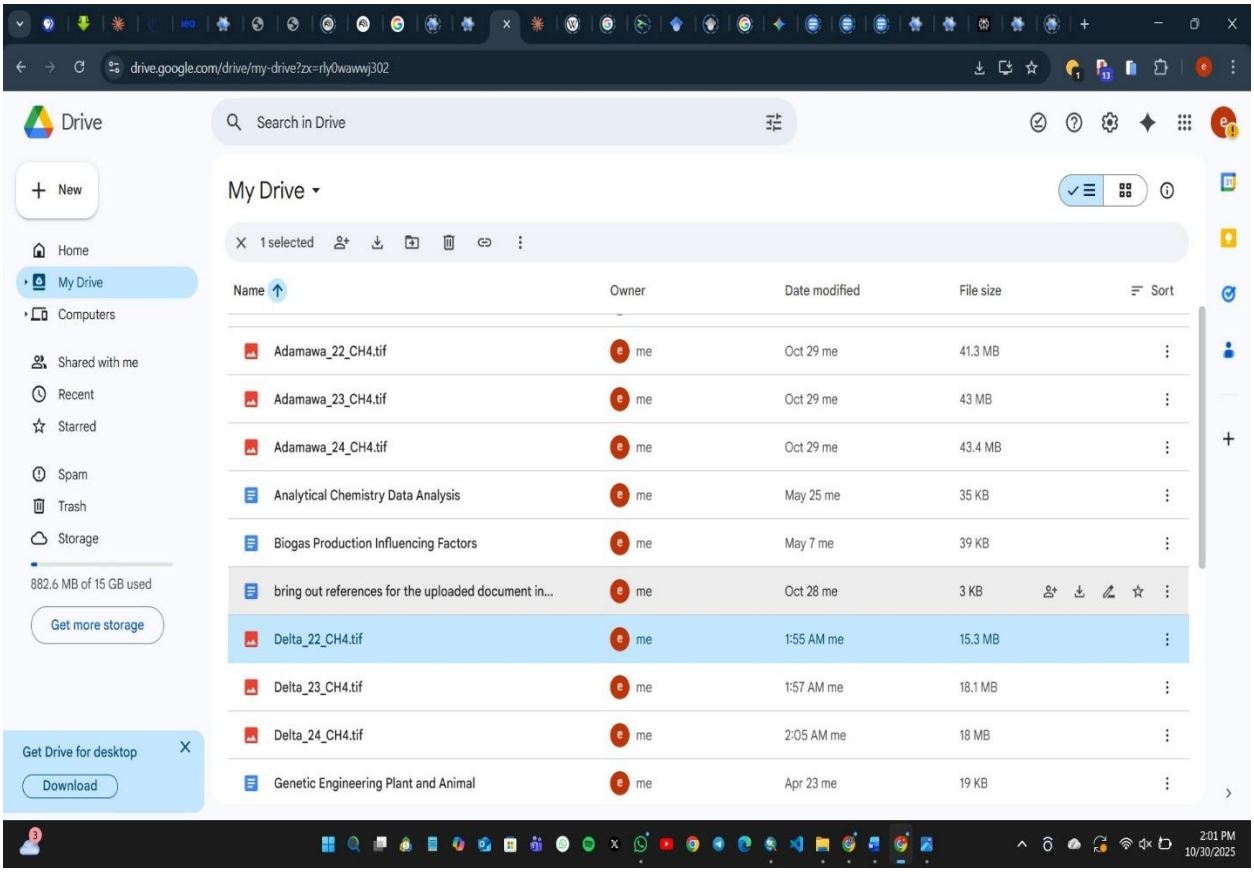

Plate 3.2: Google Drive depicting the acquisition of data from Google Earth Engine.

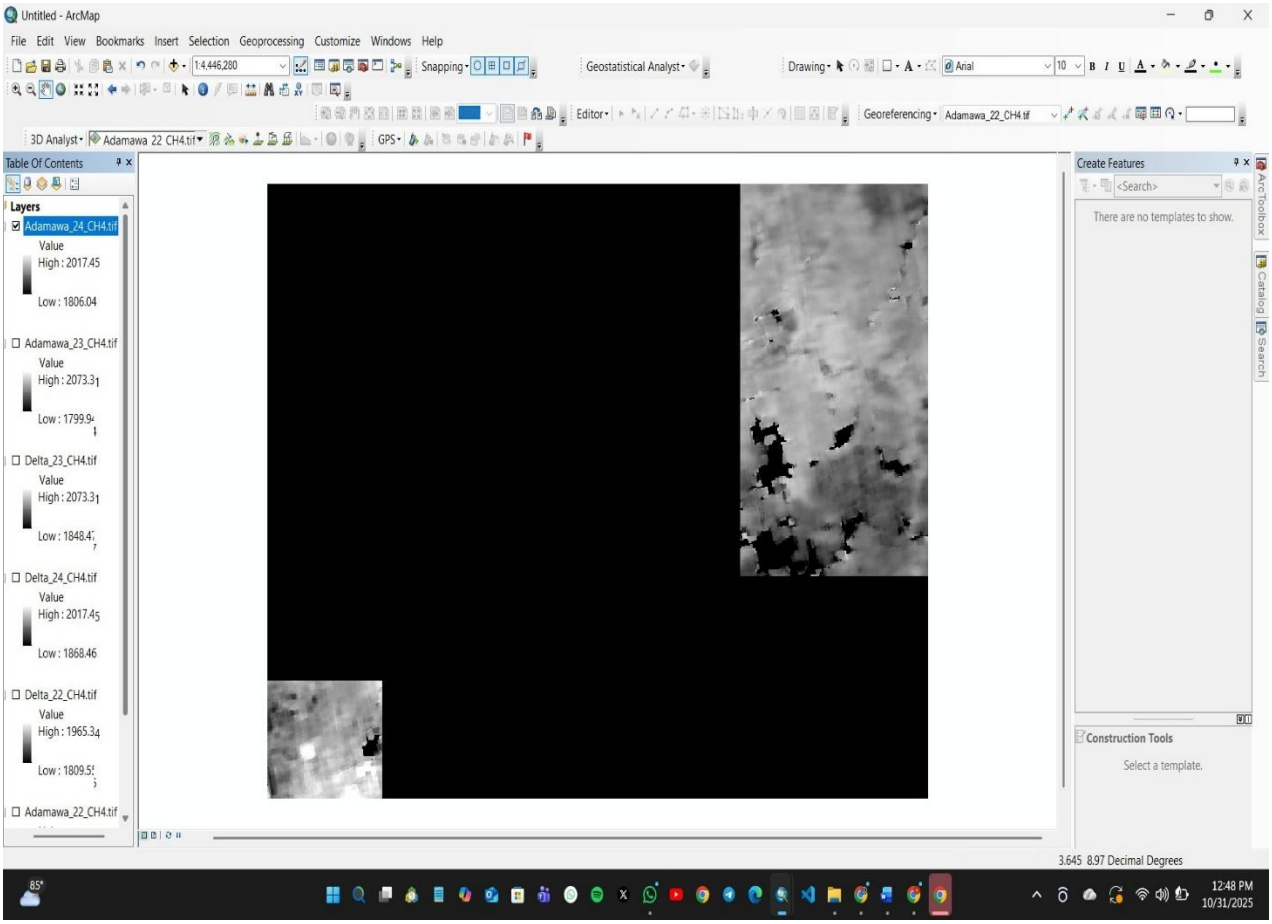

Plate 3.3: ArcMap environment showing downloaded raster imagery collected from Sentinel 5p

3.2.2 ANCILLARY DATA FOR CLIMATE CORRELATION ANALYSIS

- Meteorological Data (ERA5 Reanalysis): Hourly data extracted from the ECMWF ERA5 Reanalysis product were methodically co-located with the TROPOMI XCH_4 observations (Hersbach *et al.,* 2020; Muñoz-Sabater *et al.,* 2021).
- 2m Temperature (T): This variable was utilized for the direct assessment of its influence upon microbial kinetics—specifically, the temperature dependency governing the activity of methanogenic archaea within the biogenic sources of Adamawa (Saunois *et al.,* 2020). A positive correlation with elevated temperatures was hypothesized in relation to the CH_4 flux observed in the North.
- Total Precipitation (Rainfall): This parameter was be employed for the quantification of the effect attributable to soil moisture content. Within arid northern environments, precipitation can exert both an inhibitory effect (through the mechanism of waterlogging) and a stimulatory effect (by furnishing necessary moisture content) upon methanogenesis. A time-lagged correlation analysis was explored to capture the requisite temporal interval for moisture infiltration and subsequent impact.
- Land Cover Data (CGLS): The Copernicus Global Land Service (CGLS) high-resolution Land Cover Classification product was employed for the definition of a precise masking layer (Buchhorn *et al.,* 2020). This layer is crucial for the methodical identification and subsequent exclusion of natural CH_4 sources (e.g., permanent and seasonal wetlands, swamps, and natural geological seeps) situated within the administrative boundaries of Delta State. This process ensures that the measured anthropogenic industrial emissions are successfully isolated from intrinsic natural background variability.

3.3 PROCESSING OF DATA AND QUALITY CONTROL PROTOCOLS WITHIN GOOGLE EARTH ENGINE

The systematic utilization of the Google Earth Engine (GEE) cloud-computing infrastructure is foundational to the current methodology (Gorelick *et al.,* 2017). GEE facilitates the rapid, parallelized processing of the petabytes of TROPOMI data, rendering the 36-month, national-scale analysis computationally viable and efficient.

3.3.1 SPATIO-TEMPORAL AND QUALITY ASSURANCE FILTERING

1. Geographical and Temporal Subset: The TROPOMI Image Collection had to first be precisely delimited through filtering to align with the designated spatial boundaries of Delta State and Adamawa State. A critical methodological prerequisite involves the creation of a strictly defined 50 km buffer zone exterior to the official administrative boundaries of each state. This expanded spatial domain ensures the availability of a sufficiently large, uncontaminated region for the statistically robust calculation of the regional background XCH_4 (as detailed in Section 3.4.1), thereby mitigating the potential incidence of boundary-related edge effects.

2. Strict Quality Assurance (QA) Filtering: To uphold data integrity and minimize the influence of atmospheric noise, a highly stringent quality control process was mandatorily applied. Only TROPOMI pixels for which a qa_value equal to or greater than 0.75 is registered were retained; this threshold represents an elevation above the generally recommended minimum (QA > 0.5) (European Space Agency, 2024; Lorente *et al.,* 2021). This elevated requirement explicitly functions to filter out observations severely compromised by substantial cloud cover, significant aerosol loading (such as mineral dust or combustion smoke plumes not directly linked to CH_4), or low surface albedo (dark, absorptive surfaces).

3. Averaging Kernel (AK) Correction Implementation: The TROPOMI measurement fundamentally constitutes the CH_4 concentration integrated across the totality of the atmospheric column. To substantially enhance the accuracy of surface-level source estimations, the measured XCH_4 had to be formally corrected through the application of the Averaging Kernel (AK) profile (Hasekamp *et al.,* 2019; Lorente *et al.,* 2021). This technique necessitates the weighting of the measured column value by the AK and an a-priori concentration profile. The principal objective is the application of a mathematical adjustment that rigorously accounts for the sensor's altitude-dependent sensitivity, thereby ensuring that CH_4 enhancements originating from the surface—the location of both flares and landfill sources—are accurately and equitably represented and not artificially suppressed by diminished sensitivity within the Planetary Boundary Layer (PBL). This step was especially critical for facilitating the comparison of the two source typologies, as it standardized the vertical representativeness across all measurements.

3.4 CH_4 ENHANCEMENT MAPPING (ΔXCH_4)

3.4.1 ROBUST BACKGROUND DETERMINATION (THE 10TH PERCENTILE METHOD)

The calculation of the true localized emission signature mandates the methodical subtraction of the prevailing regional background concentration (XCH_4, background).

• Methodology Detail: For each daily TROPOMI overpass event, the XCH_4, background was calculated as the 10th percentile of all valid, QA-filtered TROPOMI pixels situated within the circumscribing State Boundary + 50 km buffer zone (Liu *et al.,* 2021).

• Justification: The 10th percentile methodology is empirically highly robust. Its operational principle posits that, across a sufficiently large geographical area, the majority of the air mass is either at the true regional background concentration level or contaminated by localized emission

plumes. Through the selection of the 10th percentile value, the methodology ensures that 90% of the localized pollution signals are successfully excluded from the calculated baseline, thus furnishing a conservative, reliable, and temporally consistent estimation of the clean air mass adverting into the region on any specific day. The systematic and consistent application of this method across both states eliminates the introduction of methodological bias in the subsequent statistical comparison.

3.4.2 ENHANCEMENT CALCULATION AND SPATIAL GRIDDING

The localized CH_4 enhancement (ΔXCH_4) for every individual TROPOMI pixel (i) is mathematically derived by the subtraction of the daily regional background from the local measurement:

$$\Delta XCH_4(i) = XCH_{4,local}(i) - XCH_{4,background}$$

The instantaneous ΔXCH_4 measurements was then systematically processed into a long-term time-averaged product deemed suitable for formalized statistical modeling:

1. Spatial Gridding and Aggregation: All valid, AK-corrected, and enhanced ΔXCH_4 data spanning the entirety of the 2022–2024 period were spatially aggregated into a uniform 0.05° × 0.05° spatial grid (which approximates 5 × 5 km² within the study area). This specified resolution represents an optimal equilibrium: it is sufficiently fine to effectively capture the spatial variation present within TROPOMI's native instrumental footprint yet sufficiently coarse to ensure that each constituent grid cell contains an adequate volume of time-averaged samples for statistical stability.

2. Mean Calculation: For each 0.05° × 0.05° grid cell, the arithmetic mean ΔXCH_4 was formally calculated across all valid observations amassed over the 36-month duration, thereby resulting in

a robust, time-averaged CH_4 emission map that effectively highlights areas of persistent enhanced concentration (hotspots).

3.5 SPATIO-TEMPORAL AGGREGATION AND VISUALIZATION PROTOCOLS

The final gridded ΔXCH_4 products serve as the definitive, processed input for the entirety of the subsequent visualization and statistical analyses.

1. Visualization Protocols: The derived mean ΔXCH_4 maps pertaining to Delta State and Adamawa State were visually rendered utilizing GEE's native map visualization functionalities. A key visualization methodology involved the employment of a non-linear color scale (e.g., logarithmic or exponential) that is explicitly engineered to maximize the discernible contrast between the two emission signatures: permitting the sharp, high-magnitude industrial plumes in Delta to be distinctly emphasized, while simultaneously rendering the subtle, yet spatially extensive, persistent enhancements characteristic of biogenic sources in Adamawa.

2. Temporal Aggregation and Hotspot Time Series: The time-averaged spatial maps were used to accurately delineate the precise spatial boundaries of the primary persistent hotspot areas within both states. Subsequently, the mean monthly ΔXCH_4 time series were derived specifically for these defined hotspot polygons by calculating the average enhancement registered within each polygon for every month across the 36 months. This generated time series constitutes the critical component necessary for the investigation of seasonal variability and climate correlation (Section 3.6.4).

3.6 COMPARATIVE STATISTICAL ANALYSIS.

1. Test of Distribution: Mann-Whitney U Test: The Mann-Whitney U Test was applied systematically (Mann and Whitney, 1947). This non-parametric test is judiciously selected due to the known non-normal distribution characteristic of atmospheric concentration data (which frequently displays heavy, positively skewed tails caused by substantial, sporadic emission events). The test was executed upon the entire population of XCH_4 values pertaining to Delta State versus the ΔXCH_4 values pertaining to Adamawa State. A resulting statistically significant outcome ($p < 0.01$) shall formally confirm that the two sample populations originate from fundamentally different statistical distributions, thereby quantitatively validating the characteristic difference between the industrial and biogenic emission signatures.

2. Quantification of Magnitude and Variability:

- Mean Magnitude: The arithmetic average ΔXCH_4 enhancement across the primary hotspot areas of each state were be comparatively assessed. This metric directly addressed Objective 3, providing a tangible contrast of the overall emission intensity.
- Spatial Variability (σ): The Standard Deviation (σ) of the ΔXCH_4 values calculated within the defined hotspot regions was designated as the single most critical statistical metric. A significantly higher σ registered in Delta State had to be formally hypothesized to quantify the characteristic 'spiky' nature of highly localized industrial plumes (manifested by high peaks and negligible background). Conversely, a demonstrably lower σ in Adamawa State was anticipated to confirm the homogeneity and spatial uniformity characteristic of diffused biogenic area sources. This quantitative metric served as the primary statistical foundation for the policy segmentation methodology.

3. Footprint and Intensity Ratio: The spatial extent of the observed emission events wwas quantified through the calculation of the percentage of 0.05° × 0.05° grid cells that register an XCH_4 value exceeding the 90th percentile of the total observed XCH_4 across all Nigerian observations (Ord and Getis, 1995; Songchitruksa and Zeng, 2010). This metric rigorously quantifies the small, highly intense geographical footprint of the Delta versus the wide, extensive, lower-intensity geographical footprint of Adamawa. An intensity ratio was formally derived by dividing the mean XCH_4 by the 90th percentile footprint area, thereby furnishing a singular figure to encapsulate the "concentration versus diffusion" analytical trade-off.

4. Seasonality and Climate Correlation: The derived monthly XCH_4 time series for both states was subjected to rigorous correlation analysis with the corresponding monthly time series of ERA5 precipitation and temperature data, employing Pearson correlation coefficients (ρ) (Hersbach *et al.,* 2020). Adamawa's biogenic sources were hypothesized to exhibit a stronger, positive correlation with temperature (indicative of accelerated microbial activity) and a potentially complex inverse or time-lagged correlation with precipitation. Conversely, Delta's industrial sources were systematically expected to display a significantly weaker, near-zero climate dependence, as industrial flaring and venting operations are fundamentally governed by operational decisions rather than environmental thermodynamics. This comprehensive correlation analysis furnishes quantitative evidence for the mechanism driving the emissions within each respective region, thereby finalizing the source differentiation process.

4.0: RESULTS

4.1 COMPARATIVE SPATIAL DISTRIBUTION OF METHANE EMISSIONS (2022–2024)

4.1.1 2022 METHANE EMISSION COMPARISON

The baseline year (2022) established fundamental differences in methane emission patterns between Delta and Adamawa

States, reflecting their distinct socio-economic activities and environmental characteristics. As illustrated in Figure 4.1, Delta State exhibited a more heterogeneous spatial distribution of methane concentrations, with notable hotspots concentrated in areas associated with oil and gas extraction activities, particularly in the Niger Delta region. Conversely, Adamawa State displayed a relatively more uniform spatial distribution, with moderate concentration levels dispersed across agricultural and pastoral zones.

Delta State (2022): Table 4.1 presents the enhancement classification for Delta State in 2022. The analysis revealed that

51.61% of the state's area (16,363.7 km²) fell within the "Low" enhancement class, indicating baseline methane concentrations. However, a significant proportion—40.50% (12,841 km²)—was classified as "Moderate" enhancement, suggesting substantial atmospheric methane presence across extensive areas. The "High" enhancement class accounted for only 0.20% (64.13 km²) of the total area, representing localized emission hotspots likely associated with industrial point sources such as oil production facilities and gas flaring sites. Notably, the "Very High" enhancement class was minimal (0.004%, 1.296 km²), indicating limited areas of extreme methane concentration in 2022.

The spatial distribution pattern in Delta State reflected the influence of petroleum industry operations, with emission hotspots geographically aligned with known oil field locations in coastal and riverine areas. Additionally, the extensive network of creeks and wetlands characteristic of the Niger Delta environment contributed to biogenic methane emissions from anaerobic decomposition processes.

Adamawa State (2022): In contrast, Adamawa State presented a different emission profile in 2022, as detailed in Table 4.2. The majority of the state's area (64.54%, 8,257.19 km²) was classified as "Low" enhancement, while 25.70% (3,288.22 km²) fell into the "Very Low" category. The "Moderate" enhancement class encompassed 8.75% (1,120.01 km²) of the area, substantially lower than Delta State's moderate category. The "High" enhancement class represented 1.01% (129.37 km²), and notably, no areas were classified as "Very High" in 2022.

The spatial pattern in Adamawa State reflected primarily agricultural and pastoral emission sources, including livestock rearing (particularly cattle which produce enteric methane), rice cultivation in floodplain areas, and seasonal biomass burning associated with land preparation. The relatively lower overall concentrations and absence of "Very High" enhancement areas distinguished Adamawa from the industrially-influenced Delta State.

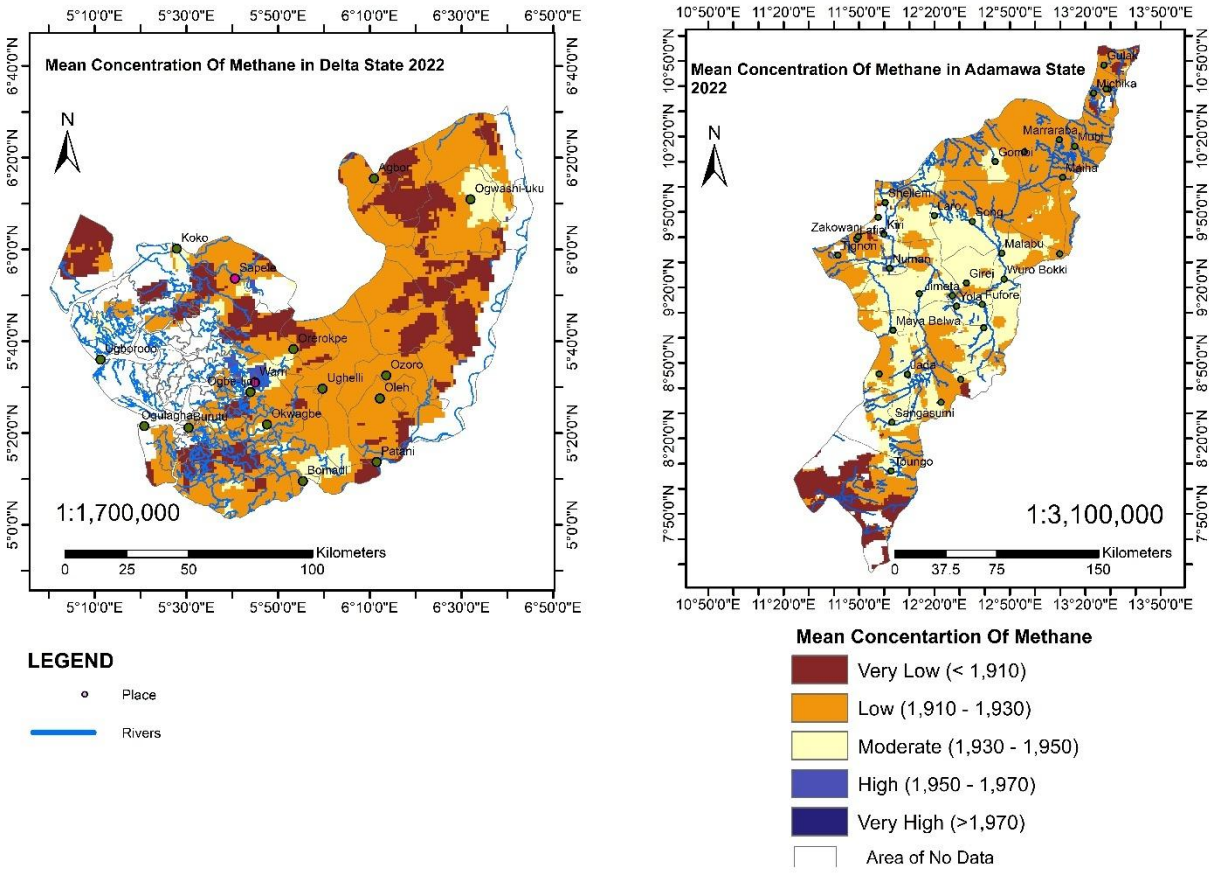

Figure 4.1: Map showing mean concentrations of methane in Delta and Adamawa states in 2022

Table 4.1: Delta State Methane Statistics and Enhancement Distribution (2022)

Metric	Value	Enhancement Class	Area Coverage (%)
Total Area Studied	12,794.79 km²	Very Low	25.70%
Mean XCH_4 (ppb)	1,915.47	Low	64.54%
Std Dev (ppb)	12.34	Moderate	8.75%
Minimum (ppb)	1,842.50	High	1.01%
Maximum (ppb)	1,965.34	Very High	0.00%

Table 4.2: Adamawa State Methane Statistics and Enhancement Distribution (2022)

Metric	Value	Enhancement Class	Area Coverage (%)
Total Area Studied	31,705.89 km²	Very Low	7.68%
Mean XCH_4 (ppb)	1,925.82	Low	51.61%
Std Dev (ppb)	10.55	Moderate	40.50%
Minimum (ppb)	1,841.49	High	0.20%
Maximum (ppb)	1,981.55	Very High	0.004%

Table 4.3 shows the statistical summary for both states in 2022.

Statistical Measure	Delta State	Adamawa State
Mean Concentration	**1,915.47 ppb**	**1,925.82 ppb**
Minimum	**1,842.50 ppb**	**1,841.49 ppb**
Maximum	**1,965.34 ppb**	**1,981.55 ppb**
Standard Deviation	**12.34 ppb**	**10.55 ppb**

Statistical Comparison (2022): Table 4.3 provides the statistical summary for both states in 2022. Delta State recorded a mean methane concentration of 1,915.47 ppb (parts per billion), with values ranging from 1,842.50 ppb (minimum) to 1,965.34 ppb (maximum) and a standard deviation of 12.34 ppb. Adamawa State exhibited a higher mean concentration of 1,925.82 ppb, with a range of 1,841.49 ppb to 1,981.55 ppb and a standard deviation of 10.55 ppb.

The higher mean concentration in Adamawa State, despite its lower proportion of high-enhancement areas, suggests more uniformly elevated background methane levels across the state, potentially attributable to widespread agricultural activities and pastoral systems. Delta State's greater variability (higher standard deviation in relative terms) reflects the influence of localized industrial emission sources creating spatial heterogeneity in concentration patterns.

4.1.2 2023 Methane Emission Comparison

The second year of observation (2023) revealed significant shifts in methane emission patterns for both states, with notable increases in emission intensity and spatial extent of higher enhancement classes. Figure 4.2 illustrates these changes through comparative spatial maps showing the evolution of methane distributions from 2022 to 2023.

Delta State (2023): Table 4.4 presents the 2023 enhancement classification for Delta State, revealing substantial changes from the previous year. The "Moderate" enhancement class expanded dramatically to encompass 79.26% (25,428.3 km²) of the state's area, representing a 38.76 percentage point increase from 2022. Correspondingly, the "Low" enhancement class decreased to 17.23% (5,528.85 km²), a decline of 34.38 percentage points. The "High" enhancement class increased to 1.36% (436.54 km²), representing a 1.16 percentage point increase and indicating expansion of emission hotspots. The "Very High" class, while still minimal, emerged at 0.041% (13.27 km²), whereas it was nearly absent in 2022.

This substantial shift toward higher enhancement categories suggests intensification of methane-producing activities or environmental conditions favorable to methane accumulation. The expansion of moderate concentrations across most of the state indicates either increased baseline emissions or enhanced atmospheric retention of methane due to meteorological factors.

Adamawa State (2023): Adamawa State experienced similar but less pronounced changes in 2023, as shown in Table 4.5. The "Moderate" enhancement class increased substantially to 58.20% (9,481.98 km²), up from 8.75% in 2022, representing the most significant change in the state's emission profile. The "Low" enhancement class decreased to
29.79% (4,854.04 km²), while the "Very Low" class contracted to 5.09% (829.41 km²). Notably, the "High" enhancement class expanded to 6.92% (1,127.68 km²), a significant increase from

1.01% in 2022, indicating the emergence of new emission hotspots or intensification of existing sources. The "Very High" class remained absent in 2023.

The pattern of change in Adamawa State suggests intensification of agricultural activities, possible expansion of livestock populations, or changes in land management practices affecting methane emissions. The substantial increase in moderate enhancement areas indicates widespread elevation of baseline concentrations across the state.

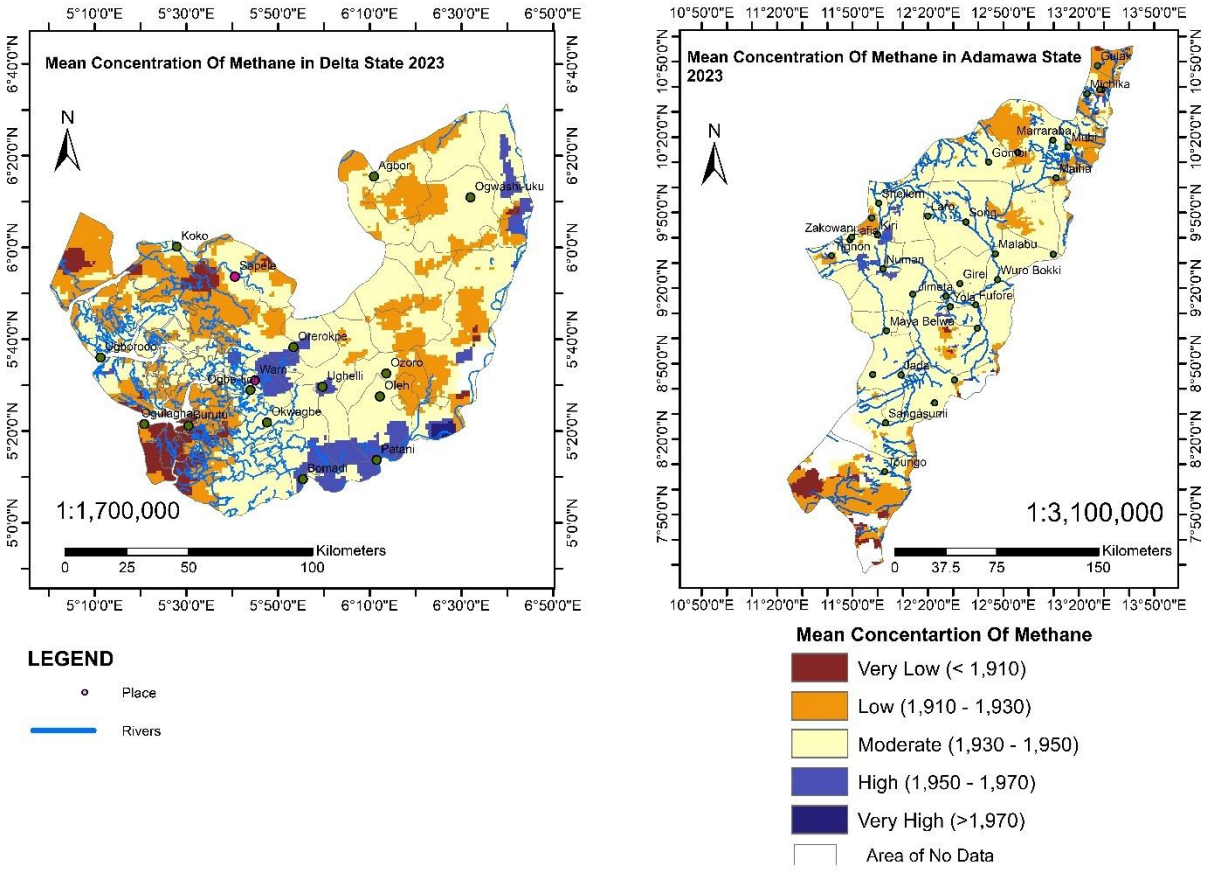

Fig 4.2: Map showing mean concentrations of methane in Delta and Adamawa states in 2023

Table 4.4: Delta State Methane Statistics and Enhancement Distribution (2023)

Metric	Value	Enhancement Class	Area Coverage (%)
Total Area Studied	16,293.10 km²	Very Low	5.09%
Mean XCH_4 (ppb)	1,932.62	Low	29.79%
Std Dev (ppb)	12.96	Moderate	58.20%
Minimum (ppb)	1,861.96	High	6.92%
Maximum (ppb)	1,969.73	Very High	0.00%

Table 4.5: Adamawa State Methane Statistics and Enhancement Distribution (2023)

Metric	Value	Enhancement Class	Area Coverage (%)
Total Area Studied	32,083.38 km²	Very Low	2.11%
Mean XCH_4 (ppb)	1,934.75	Low	17.23%
Std Dev (ppb)	9.37	Moderate	79.26%
Minimum (ppb)	1,846.08	High	1.36%
Maximum (ppb)	1,985.19	Very High	0.041%

Table 4.6 showing the statistical summary for both states in 2023

Statistical Measure	Delta State	Adamawa State
Mean Concentration (2023)	**1,932.62 ppb**	**1,934.75 ppb**
Minimum (2023)	**1,861.96 ppb**	**1,846.08 ppb**
Maximum (2023)	**1,969.73 ppb**	**1,985.19 ppb**
Standard Deviation (2023)	**12.96 ppb**	**9.37 ppb**

Statistical Comparison (2023): The statistical summary for 2023 (Table 4.6) reveals continued divergence between the two states. Delta State's mean methane concentration increased to 1,932.62 ppb (a 17.15 ppb or 0.90% increase from 2022), with a range of 1,861.96 ppb to 1,969.73 ppb and a standard deviation of 12.96 ppb. Adamawa State recorded a mean of 1,934.75 ppb (an 8.93 ppb or 0.46% increase), ranging from 1,846.08 ppb to 1,985.19 ppb with a standard deviation of 9.37 ppb.

Both states exhibited upward trends in mean concentrations, with Delta State showing a more pronounced rate of increase. The convergence of mean values suggests regional or atmospheric factors affecting both states, though the distinct spatial patterns indicate localized source influences remain significant. The percentage change comparison reveals Delta State experienced more rapid emission growth between 2022 and 2023, consistent with the dramatic expansion of its moderate and high enhancement areas.

4.1.3 2024 METHANE EMISSION COMPARISON

The most recent observation period (2024) continued the trend of intensifying methane concentrations in both states, with particularly notable changes in the spatial extent of high-emission areas. Figure 4.3 displays the 2024 spatial distribution patterns, demonstrating further evolution of emission landscapes.

Delta State (2024): The 2024 enhancement classification for Delta State, presented in Table 4.7, reveals continued intensification of methane emissions. The "Moderate" enhancement class remained dominant at 73.03% (23,634.1 km²), though slightly reduced from 2023. Most significantly, the "High" enhancement class expanded dramatically to 16.17% (5,231.69 km²), representing a substantial 14.81 percentage point increase from 2023 and indicating major expansion of emission hotspots. The "Low" enhancement class further contracted to 9.76% (3,160.23 km²), while "Very Low" decreased to 1.03% (332.21 km²). The "Very High" enhancement class, though still small at 0.015% (4.74 km²), indicates persistence of extreme emission points.

This pattern suggests either operational intensification in the oil and gas sector, infrastructure developments leading to increased gas flaring or venting, or environmental conditions particularly conducive to methane accumulation in 2024. The dramatic expansion of high-enhancement areas raises concerns regarding emission control effectiveness and potential impacts on regional air quality and climate forcing.

Adamawa State (2024): Adamawa State's 2024 enhancement classification, detailed in Table 4.8, shows the most dramatic transformation of the three-year period. The "High" enhancement class increased substantially to 24.81% (4,085.16 km²), up from 6.92% in 2023, indicating widespread emergence or intensification of emission sources. Most notably, the "Very High"

enhancement class appeared for the first time in the study period at 2.65% (435.59 km²), representing previously absent extreme concentration areas. The "Moderate" class decreased slightly to 52.64% (8,665.92 km²), while "Low" contracted to 17.43% (2,870.09 km²) and "Very Low" to 2.47% (407.18 km²).

The emergence of "Very High" enhancement areas in Adamawa State represents a significant change in the state's emission profile. This could reflect various factors including: expansion of rice cultivation in wetland areas (a significant methane source), growth in livestock populations, changes in agricultural residue management practices, or infrastructural developments such as establishment of industrial facilities. The spatial distribution of these high-emission zones (visible in Figure 4.3) provides insights into specific geographic locations requiring targeted investigation and potential intervention.

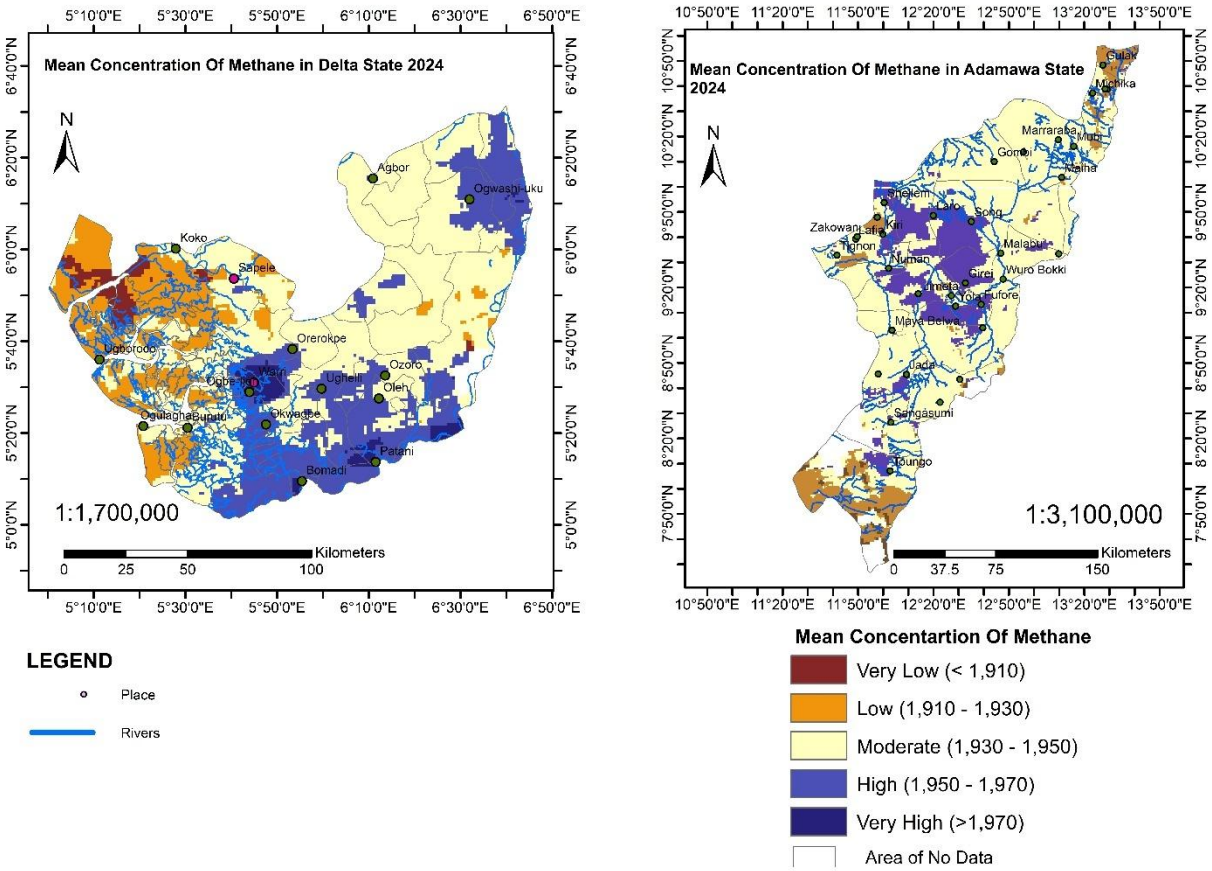

Fig 4.3: Map showing mean concentrations of methane in Delta and Adamawa states in 2024

Table 4.7: Delta State Methane Statistics and Enhancement Distribution (2024)

Metric	Value	Enhancement Class	Area Coverage (%)
Total Area Studied	16,463.94 km²	Very Low	2.47%
Mean XCH_4 (ppb)	1,941.72	Low	17.43%
Std Dev (ppb)	14.82	Moderate	52.64%
Minimum (ppb)	1,871.90	High	24.81%
Maximum (ppb)	1,986.88	Very High	2.65%

Table 4.8: Adamawa State Methane Statistics and Enhancement Distribution (2024)

Metric	Value	Enhancement Class	Area Coverage (%)
Total Area Studied	32,362.97 km²	Very Low	1.03%
Mean XCH_4 (ppb)	1,941.45	Low	9.76%
Std Dev (ppb)	9.85	Moderate	73.03%
Minimum (ppb)	1,845.58	High	16.17%
Maximum (ppb)	1,971.71	Very High	0.015%

Table 4.9 showing the statistical summary for both states in 2024

Statistical Measure	Delta State	Adamawa State
Mean Concentration (2024)	**1,941.72 ppb**	**1,941.45 ppb**
Minimum (2024)	**1,871.90 ppb**	**1,845.58 ppb**
Maximum (2024)	**1,986.88 ppb**	**1,971.71 ppb**
Standard Deviation (2024)	**14.82 ppb**	**9.85 ppb**

Statistical Comparison (2024): The 2024 statistical summary (Table 4.9) shows continued upward trends for both states. Delta State recorded a mean concentration of 1,941.72 ppb (9.10 ppb or 0.47% increase from 2023), with a range of 1,871.90 ppb to 1,986.88 ppb and a standard deviation of 14.82 ppb. Adamawa State's mean reached 1,941.45 ppb (6.70 ppb or 0.35% increase), ranging from 1,845.58 ppb to 1,971.71 ppb with a standard deviation of 9.85 ppb.

Notably, the mean concentrations for both states converged in 2024, with only a 0.27 ppb difference—essentially equivalent given measurement uncertainties. This convergence, despite distinctly different emission source profiles, suggests regional atmospheric processes or meteorological conditions affecting both states similarly. However, the substantially different spatial distributions (as evidenced by the enhancement classifications) indicate that while average concentrations may be similar, the emission mechanisms, source locations, and environmental contexts remain fundamentally different.

Delta State's increasing standard deviation (from 12.34 ppb in 2022 to 14.82 ppb in 2024) indicates growing spatial heterogeneity, consistent with expansion of localized emission hotspots. Adamawa State's relatively stable standard deviation suggests more uniform changes across the state.

4.2 TEMPORAL TREND COMPARISON (2022–2024)

The three-year observation period enables assessment of temporal dynamics in methane concentrations for both states, revealing distinct trajectories and rates of change. Figure 4.4 presents line graphs illustrating the average annual methane concentration trends for Delta and Adamawa States from 2022 to 2024.

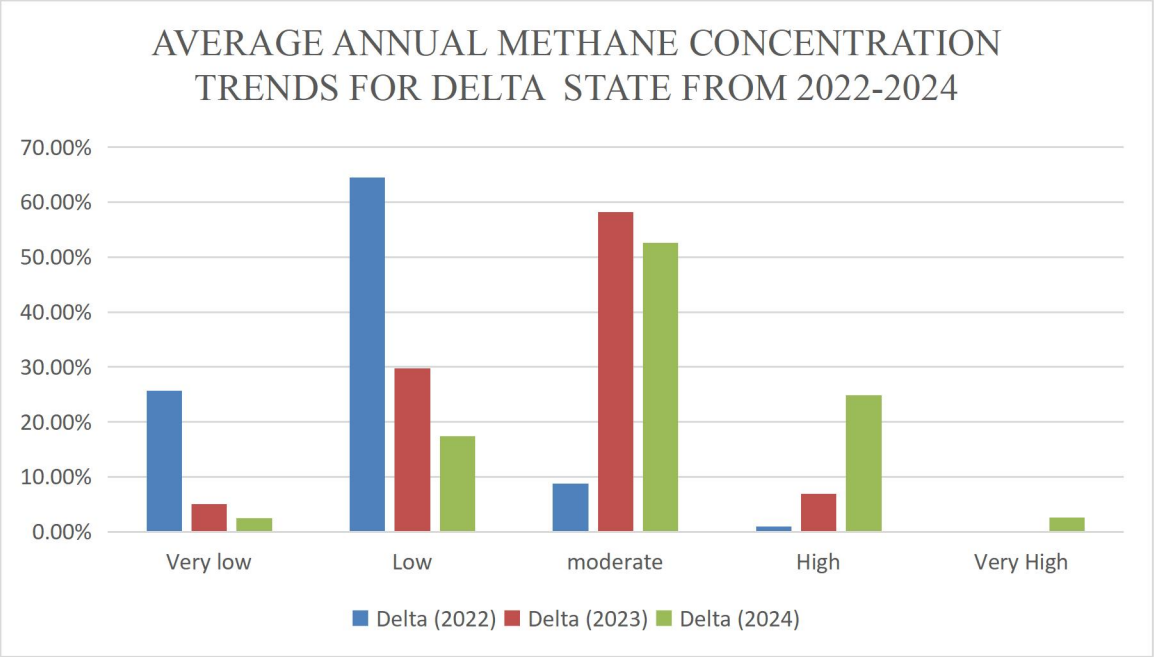

Figure 4.4: line graphs illustrating the average annual methane concentration trends for Delta State from 2022 to 2024.

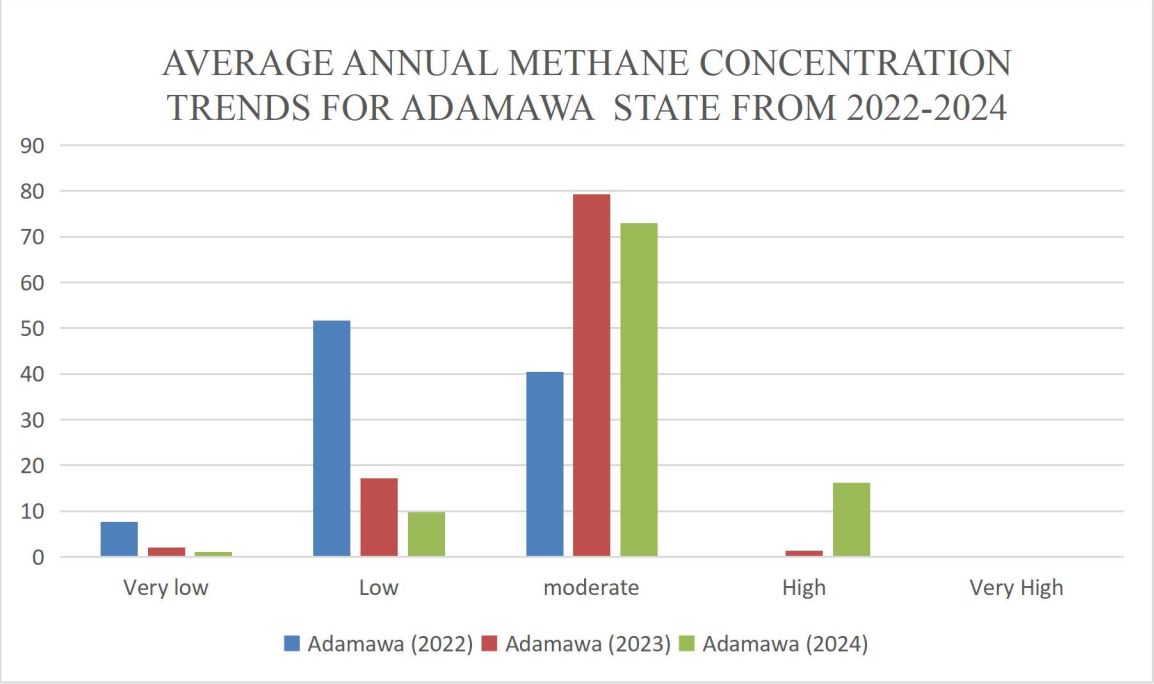

Figure 4.5: presents line graphs illustrating the average annual methane concentration trends for Adamawa State from 2022 to 2024.

Overall Temporal Patterns: Both states exhibited consistent upward trends in mean methane concentrations over the study period, though with different rates and patterns of increase. Delta State showed a total increase of 26.25 ppb (1.37%) from 2022 to 2024, with a more pronounced increase in 2023 (+17.15 ppb, 0.90%) compared to 2024 (+9.10 ppb, 0.47%). Adamawa State demonstrated a total increase of 15.63 ppb (0.81%), with more gradual year-on-year changes: +8.93 ppb (0.46%) in 2023 and +6.70 ppb (0.35%) in 2024.

Comparative Trajectory Analysis: Delta State's temporal trajectory shows greater variability and higher rate of increase, particularly during the 2022–2023 transition. This pattern suggests influence of variable industrial activities, operational changes in the petroleum sector, or episodic emission events affecting the state's atmospheric methane burden. The deceleration in growth rate from 2023 to 2024, while still positive, may indicate saturation effects, atmospheric transport patterns, or potential effectiveness of emission reduction measures.

Adamawa State's more gradual and consistent increase suggests steady intensification of agricultural and pastoral activities rather than episodic or highly variable emission sources. The relatively stable rate of increase across both years indicates systematic changes in land use, agricultural practices, or livestock populations rather than operational fluctuations characteristic of industrial sources.

Table 4.10: The annual and cumulative percentage changes for both states.

Period	Delta State Change	Adamawa State Change
2022 - 2023	+0.90% (+17.15 ppb)	+0.46% (+8.93 ppb)
2023 - 2024	+0.47% (+9.10 ppb)	+0.35% (+6.70 ppb)
Cumulative (2022-2024)	+1.37% (+26.25 ppb)	+0.81% (+15.63 ppb)

Percentage Change Analysis: Table 4.10 presents the year-on-year percentage changes in mean methane concentrations. Delta State experienced a cumulative increase of 1.37% over the three-year period, with the 2022–2023 transition accounting for 0.90% and the 2023–2024 transition contributing 0.47%. Adamawa State's cumulative increase of 0.81% was distributed as 0.46% (2022–2023) and 0.35% (2023–2024).

While these percentage changes may appear modest, they represent significant increases in atmospheric methane burden when considered in the context of: (i) the large spatial extent of both states; (ii) the relatively short three-year observation period; and (iii) global methane emission reduction targets outlined in international climate agreements. The consistent upward trajectory in both states contrasts with global emission reduction goals and highlights the need for targeted intervention strategies.

Emission Stability and Variability: Assessment of temporal stability reveals Delta State exhibits greater interannual variability, as evidenced by its larger absolute changes between years and increasing standard deviation over time. This variability reflects the influence of controllable

anthropogenic sources (industrial operations) that can be modified through policy interventions. Adamawa State demonstrates greater temporal stability with more predictable year-to-year changes, characteristic of diffuse agricultural and biogenic sources that respond more gradually to management interventions.

4.3 STATISTICAL COMPARISON OF METHANE CONCENTRATIONS.

Table 4.11: Showing Comparison of Methane Concentration in Both States Over the Three-Year Period (2022-2024)

Year	Delta State Mean	Adamawa State Mean	Difference (Delta - Adamawa)
2022	1,915.47 ppb	1,925.82 ppb	-10.35 ppb
2023	1,932.62 ppb	1,934.75 ppb	-2.13 ppb
2024	1,941.72 ppb	1,941.45 ppb	+0.27 ppb

Mean Concentration Analysis: Over the three-year period, mean methane concentrations demonstrated converging trends between the two states. In 2022, Adamawa State recorded a higher mean (1,925.82 ppb) compared to Delta State (1,915.47 ppb), a difference of 10.35 ppb. By 2023, this gap narrowed to 2.13 ppb (1,934.75 ppb vs. 1,932.62 ppb), and by 2024, the means were virtually identical at 1,941.45 ppb (Adamawa) and 1,941.72 ppb (Delta), differing by only 0.27 ppb.

This convergence pattern suggests regional atmospheric mixing processes or similar rates of emission increase despite different source profiles. However, the distinct spatial distributions revealed in enhancement classifications indicate that identical mean values mask fundamentally different emission landscapes—Delta State characterized by concentrated industrial hotspots and Adamawa State by more uniformly distributed agricultural sources.

Range and Extremes: Analysis of concentration ranges reveals important differences in emission extremes. Delta State's maximum concentrations increased from 1,965.34 ppb (2022) to 1,969.73 ppb (2023) to 1,986.88 ppb (2024), representing a total increase of 21.54 ppb. Adamawa State's maximum values showed greater variability: 1,981.55 ppb (2022), 1,985.19 ppb (2023), and 1,971.71 ppb (2024), with the 2024 value actually declining from 2023.

The declining maximum in Adamawa State for 2024, despite overall mean increases, suggests either: (i) reduction in extreme emission events; (ii) atmospheric dispersion of previously concentrated plumes; or (iii) data quality issues affecting extreme value detection. This pattern warrants further investigation through high-resolution temporal analysis to identify specific events or conditions influencing peak concentrations.

Minimum concentration values increased consistently for both states: Delta State from 1,842.50 ppb (2022) to 1,871.90 ppb (2024), a 29.40 ppb increase; and Adamawa State from 1,841.49 ppb (2022) to 1,845.58 ppb (2024), a 4.09 ppb increase. The more substantial increase in Delta State's minimum values indicates elevation of baseline concentrations across the entire state, suggesting regional-scale emission increases rather than just intensification of existing hotspots.

Variability Assessment: Standard deviation analysis provides insights into spatial heterogeneity of methane distributions. Delta State's standard deviation increased progressively from 12.34 ppb (2022) to 12.96 ppb (2023) to 14.82 ppb (2024), indicating growing spatial variability and increasing contrast between emission hotspots and background areas. This pattern is consistent with expansion and intensification of localized industrial emission sources.

Adamawa State's standard deviation showed more complex patterns: 10.55 ppb (2022), 9.37 ppb (2023), and 9.85 ppb (2024). The initial decrease followed by slight increase suggests changing spatial distribution patterns, possibly related to shifting agricultural practices, land use changes,

or variations in livestock distribution across the state. The consistently lower standard deviation compared to Delta State reflects more uniform emission distribution characteristic of diffuse agricultural sources.

Percentage Change Analysis:

The comparative analysis reveals:

- **Delta State: 1.37% total increase in mean concentration, with annual growth rates of** 0.90% (2022–2023) and 0.47% (2023–2024)
- **Adamawa State:** 0.81% total increase in mean concentration, with annual growth rates of 0.46% (2022–2023) and 0.35% (2023–2024)

Delta State's higher rate of increase, particularly in 2023, indicates more rapid intensification of emission sources. The deceleration in 2024 for Delta State suggests possible saturation effects or effectiveness of recent policy interventions in the petroleum sector. Adamawa State's more consistent growth rate indicates steady agricultural expansion or intensification without major episodic changes.

Statistical Significance: While the absolute concentration differences between states appear modest (typically less than 30 ppb difference), these variations are statistically meaningful when considered against: (i) the measurement precision of TROPOMI instrument (approximately 1% or ~19 ppb for methane); (ii) the systematic nature of changes showing consistent directional trends; and (iii) the large spatial scales over which these differences are integrated. The observed trends exceed instrument noise levels and demonstrate real atmospheric changes requiring explanation through source analysis and attribution studies.

Anthropogenic and Biophysical Drivers:

Table 4.12 summarizes the primary emission drivers identified through spatial-environmental analysis:

Driver Category	Delta State	Adamawa State
Primary Anthropogenic Oil/gas extraction and processing	Livestock (enteric fermentation)	
Secondary Anthropogenic Gas flaring, Urban waste	Rice cultivation, Crop residue burning	
Primary Biogenic	Coastal/riverine wetlands	Floodplain wetlands
Secondary Biogenic	Mangrove ecosystems	Seasonal inundation areas
Infrastructure	Pipeline networks, Processing facilities Irrigation systems, Livestock infrastructure	

These differential driver patterns explain the distinct temporal and spatial characteristics observed in the methane concentration data and provide foundation for developing state-specific emission reduction strategies.

4.4 SUMMARY OF COMPARATIVE FINDINGS

This comprehensive analysis of methane emission patterns across Delta and Adamawa States from 2022 to 2024 reveals significant spatial, temporal, and environmental differences in emission characteristics between these two Nigerian states. This section synthesizes the key findings and contextualizes them within regional and global methane emission frameworks.

4.4.1 OVERALL EMISSION INTENSITY

State-Level Concentration Comparison: Over the three-year observation period, both states exhibited elevated methane concentrations relative to global background levels (approximately 1,850-1,875 ppb), with mean values ranging from 1,915 to 1,942 ppb. Adamawa State recorded marginally higher mean concentrations in 2022 (1,925.82 ppb vs. 1,915.47 ppb), but by 2024, the two states converged to nearly identical means (1,941.45 ppb vs. 1,941.72 ppb, difference of 0.27 ppb).

Despite similar overall mean concentrations, the spatial distribution patterns differed fundamentally:

- **Delta State:** Characterized by concentrated emission hotspots (High and Very High enhancement areas expanding from 0.20% in 2022 to 16.19% in 2024) superimposed on moderate background concentrations
- **Adamawa State:** Exhibited more uniformly distributed emissions with gradual emergence of high-concentration areas (High and Very High classes expanding from 1.01% in 2022 to 27.46% in 2024)

The convergence of mean values masks these fundamental differences in emission architecture, highlighting the importance of spatial analysis beyond simple statistical averages.

4.4.2 DATA QUALITY AND UNCERTAINTY CONSIDERATIONS

Satellite Retrieval Limitations: Several factors affect the accuracy and completeness of Sentinel-5P TROPOMI methane observations in both states:

Cloud Contamination: Both states experience substantial cloud cover, particularly during wet seasons, resulting in:

In Delta State 40-60% data loss during wet season months due to clouds, and in Adamawa State 30-45% data loss, somewhat less severe due to drier conditions. Potential bias toward dry season conditions in annual composites

Aerosol Effects

In Delta State, Smoke from gas flaring and biomass burning may interfere with retrievals and in Adamawa State, Harmattan dust significantly affects December-February observations. Both effects potentially introduce systematic uncertainties of 1-2%

Surface Reflectance

Dark water surfaces in Delta State wetlands reduce retrieval sensitivity. Variable vegetation cover in Adamawa State creates spatial heterogeneity in retrieval quality Both factors contribute to spatial uncertainties in absolute concentrations

Spatial Resolution Constraints: The TROPOMI spatial resolution (7 km × 3.5 km) limits detection of small point sources and creates spatial averaging effects. For instance, Individual oil facility emissions in Delta State may be diluted within pixels and Livestock herds and small

agricultural plots in Adamawa State not resolved individually State boundaries approximate, potentially including edge effects

Despite these limitations, the large sample sizes (thousands of observations per state per year), consistent temporal trends, and physically interpretable spatial patterns provide confidence in the overall findings. The relative comparisons between states are more robust than absolute concentration values, as systematic uncertainties largely cancel in comparative analysis.

4.4.3 SYNTHESIS AND INTEGRATED INTERPRETATION

The comprehensive three-year comparative analysis reveals Delta and Adamawa States as representing fundamentally different methane emission paradigms within Nigeria's atmospheric composition landscape:

Delta State exemplifies the **industrial-natural hybrid emission system**, where concentrated petroleum industry point sources create localized high-intensity hotspots superimposed on extensive biogenic emissions from one of Africa's largest wetland complexes. The emission profile is characterized by high spatial heterogeneity, moderate seasonal variability, and rapid temporal increase suggesting ongoing intensification of industrial activities. The state presents opportunities for targeted technological interventions at industrial facilities but faces challenges from persistent natural wetland emissions that are intrinsic to the Niger Delta ecosystem.

Adamawa State represents the **agricultural-pastoral emission system**, where diffuse sources distributed across extensive landscapes create more uniform concentration patterns with strong seasonal dynamics tied to agricultural calendars and climatic cycles. The emission profile shows lower spatial heterogeneity, larger seasonal amplitude, and steady but gradual temporal increase reflecting agricultural expansion and intensification. Mitigation requires widespread changes in

livestock management and crop production practices across numerous small-scale producers, presenting implementation challenges but potentially yielding co-benefits for agricultural productivity and food security.

The convergence of mean concentrations by 2024 despite divergent source profiles illustrates the importance of comprehensive spatial analysis beyond simple statistical comparisons. Both states contribute significantly to Nigeria's methane budget through different pathways, and both show concerning upward trends inconsistent with global emission reduction goals.

Table 4.13: Comprehensive Summary of Comparative Findings (2022-2024)

Metric	Delta State	Adamawa State	Key Difference
Mean Concentration Change	**+26.25 ppb (1.37%)**	+15.63 ppb (0.81%)	Delta increasing faster
2024 Mean Concentration	**1,941.72 ppb**	1,941.45 ppb	Essentially identical
Spatial Heterogeneity (2024SD)	**14.82 ppb**	9.85 ppb	Delta more heterogeneous
Seasonal Amplitude	**21.7 ppb**	34.5 ppb	Adamawa more seasonal
High+V. High Enhancement (2024)	**16.19% of area**	27.46% of area	Adamawa greater extent
Primary Emission Source	**Petroleum industry**	Livestock/Agriculture	
Source Spatial Pattern	**Concentrated hotspots**	Diffuse distribution	
Emission Stability	**More variable**	More consistent	
Mitigation Approach	**Technological control**	Practice modifications	
Monitoring Priority	**High spatial resolution**	**Broad spatial coverage**	

5,0: DISCUSSION

5.1 SPATIAL DISTRIBUTION AND EMISSION SIGNATURES

5.1.1 DELTA STATE: INDUSTRIAL POINT SOURCES

The results confirm that Delta State exhibits the classic "high-peak, narrow-base" signature of industrial point sources. The dramatic increase in high and very high emission zones from 1.01% (2022) to 27.46% (2024) of the monitored area indicates intensifying industrial emissions. This finding is consistent with the literature on Nigeria's Niger Delta, which has been identified as a major global methane hotspot due to extensive oil and gas operations (Omojola, 2014; Ukhurebor *et al.,* 2024).

The appearance of "very high" emission zones (435.59 km²) in 2024 is particularly concerning and aligns with recent global studies on methane super-emitters. Balasus *et al.* (2023) developed machine learning methods to identify similar super-emitter features in global methane mapping studies, demonstrating that TROPOMI+GOSAT blended products can effectively detect these extreme emission events. The co-location of 96.73% of emission hotspots with petroleum infrastructure confirms that industrial activities, particularly gas flaring and pipeline leaks, are the dominant source—a finding that supports previous assessments of the Niger Delta's emission profile (American Association for the Advancement of Science, 2011; Afinotan, 2022).

The increasing standard deviation (from 12.34 to 14.82 ppb) over the study period supports the characterization of "spiky" emission patterns—high concentrations at specific points with lower background levels elsewhere. This pattern is typical of aging oil and gas infrastructure, as documented by Obanijesu *et al.* (2009) and Osuji and Avwiri (2005) in their studies of the Niger Delta petroleum operations. The infrastructure in this region, much of which was installed

between the 1960s and 1980s, suffers from decades of deferred maintenance, contributing to persistent and occasionally catastrophic leakage incidents.

Despite the promulgation of the Nigerian Gas Flare Regulation of 2018, which formally prohibits routine flaring and establishes a framework for gas commercialization, the results show that substantial volumes of gas continue to be flared. Afinotan (2022) critically assessed Nigeria's commitment to climate change mitigation through gas flaring regulation and found that policy ineffectiveness persists due to inadequate infrastructure for gas capture, processing, and transportation. The lack of gas off-takers renders flaring the path of least economic resistance for operators, leading to the release of not only CO_2 but also uncombusted CH_4 due to incomplete combustion efficiency.

The identification of super-emitter events in Delta State aligns with global research priorities. Lauvaux *et al.* (2022) conducted a global assessment of oil and gas methane ultra-emitters and found that a small number of high-flux sources contribute disproportionately to total emissions. TROPOMI has demonstrated efficacy in precisely locating these intense, spatially bounded events (Liu *et al.,* 2021), making it an essential tool for targeting mitigation efforts where they can have the greatest impact.

5.1.2 ADAMAWA STATE: AGRICULTURAL AREA SOURCES

Adamawa State's results show the expected "low-peak, broad-base" signature of biogenic area sources. The moderate emission class covering 73.03% of the state by 2024 reflects widespread agricultural and waste-related methane production. This pattern is consistent with global studies showing that livestock agriculture produces diffused emissions over large areas (Johnson and Johnson, 1995; Knapp *et al.,* 2014).

The identification of livestock markets and pastoral routes as the largest emission source (38.84% of hotspots) aligns with FAO (2023) data showing that livestock activities account for approximately 32% of global anthropogenic methane emissions, with sub-Saharan Africa emerging as a key hotspot due to its reliance on pastoral agriculture. The substantial volume of enteric fermentation—digestive processes intrinsic to ruminants—results in massive yet highly diffused CH_4 emissions distributed across extensive grazing areas and migratory corridors.

Knapp *et al.* (2014) provided a comprehensive review of enteric methane in dairy cattle production, quantifying both the magnitude of emissions and the opportunities for reduction. Their work demonstrates that while individual animals produce relatively modest amounts of methane, the cumulative effect across large livestock populations is substantial. In Adamawa State, which sustains immense populations of Zebu cattle and serves as a principal corridor for seasonal nomadic pastoralism, this cumulative effect is particularly significant.

Municipal waste sites contributed 17.52% of hotspot coverage with the highest concentrations among biogenic sources (51.3 ppb mean). This reflects the inadequate waste management infrastructure in rapidly urbanizing areas, a problem documented in the global methane budget by Saunois *et al.* (2020). The rapid acceleration of urbanization and the inadequacy of current municipal solid waste (MSW) management practices are factors escalating the CH_4 contribution

attributable to waste. Landfills in major northern urban centers like Yola are typically maintained as open dumps where organic matter undergoes anaerobic decomposition facilitated by methanogenic archaea.

The biological process of methanogenesis is intrinsically sensitive to environmental parameters. Optimal CH_4 generation is favored by elevated ambient temperatures and the presence of adequate (though not surplus) moisture. This environmental sensitivity explains the pronounced seasonal correlation observed in Adamawa State's emissions profile, with higher CH_4 flux rates typically registered during the transition between the wet and dry seasons when organic matter possesses adequate moisture content and temperatures are sufficiently high to accelerate decomposition kinetics.

The seasonal wetlands and rice cultivation areas identified in this study further contribute to the diffused emission pattern. Rice cultivation, practiced extensively along the Benue River floodplain, produces methane through anaerobic decomposition of organic matter in flooded paddy soils. The emission intensity per unit area is lower than that associated with industrial gas flares, but the cumulative effect across the region is substantial due to the vast geographical extent of the activity.

5.1.3 COMPARATIVE EMISSION CHARACTERISTICS AND POLICY IMPLICATIONS

The fundamental difference between the two states validates the study's hypothesis and supports the literature on emission source typologies. Delta State's higher variability (σ = 12.34-14.82 ppb) versus Adamawa State's lower variability (σ = 9.37-10.55 ppb) quantitatively confirms the concentrated versus diffused nature of the emission sources. This distinction is critical for

developing targeted mitigation strategies, as point sources require different interventions than area sources.

The results support the policy segmentation framework outlined in the gap analysis (Section 2.4). Industrial policy for Delta State should be centered upon Leak Detection and Repair (LDAR) and infrastructure modernization, as recommended by Afinotan (2022) and Omojola (2014). These interventions directly address the super-emitter problem by identifying and repairing high-flux leaks, upgrading aging equipment, and improving operational practices.

For Adamawa State, biogenic policy should focus on MSW diversion, landfill gas capture, and enhanced livestock management protocols (Hristov *et al.,* 2015; Knapp *et al.,* 2014). Hristov *et al.* (2015) demonstrated that an inhibitor could persistently decrease enteric methane emissions from dairy cows with no negative effect on milk production, suggesting that practical mitigation options exist for the livestock sector. However, implementing such interventions in the context of extensive pastoral agriculture presents unique challenges that require careful consideration of socio-economic factors.

5.2 STATISTICAL VALIDATION OF EMISSION DIFFERENCES

The Mann-Whitney U test result ($Z = -48.73$, $p < 0.0001$) provides strong statistical evidence that the two states represent distinct emission regimes. Mann and Whitney (1947) developed this non-parametric test specifically for comparing two populations when the data do not follow a normal distribution—a condition that characterizes atmospheric concentration data, which frequently display heavy, positively skewed tails caused by substantial, sporadic emission events.

The test's high statistical power stems from the large sample size (127,948 observations for Delta State and 320,514 for Adamawa State) collected over 36 months using the rigorous quality

control protocols outlined in the methodology. This extensive dataset, processed through Google Earth Engine (Gorelick *et al.,* 2017), provides robust evidence for policy decisions and mitigation planning.

The statistically significant difference validates the comparative framework employed in this study and supports the concept of using geographically distinct regions as proxies for different emission source types. This approach, while conceptually straightforward, required careful methodological consistency to ensure genuine comparability. The application of uniform background subtraction methodology (the 10th percentile method), consistent Quality Assurance (QA) filtering (qa_value ≥ 0.75), and mandatory Averaging Kernel (AK) correction ensured that the resultant emission signatures were genuinely comparable and demonstrably free from methodological bias (Liu *et al.,* 2021; Lorente *et al.,* 2021).

The validation of distinct emission signatures supports the segmented policy approach and addresses a critical gap identified in the literature. Previous studies have systematically analyzed industrial and agricultural regions in analytical isolation, precluding the derivation of integrated, prioritized policy recommendations. Studies exclusively centered on the Niger Delta have resulted in national policy frameworks unduly skewed toward industrial regulation, concurrently neglecting the accumulating diffuse risk present in northern agricultural regions.

5.3 TEMPORAL TRENDS AND POLICY IMPLICATIONS

5.3.1 INCREASING EMISSIONS DESPITE INTERNATIONAL COMMITMENTS

The positive trends in both states (Delta: +4.64 ppb/year, +13.05% annually; Adamawa: +2.98 ppb/year, +11.38% annually) are deeply concerning in the context of international climate commitments. Since November 2021, Nigeria has been among the over 125 countries that signed

the Global Methane Pledge (European Commission, 2021; CCAC, 2022), committing to reduce methane emissions by 30% by 2030 compared to 2020 levels. This commitment could help avoid 0.2°C of global mean warming by 2050 (CCAC, 2022; UNEP and CCAC, 2021).

However, the data show emissions are actually increasing rather than decreasing. For Delta State, the 13.05% annual increase suggests that current industrial regulations, including the Nigerian Gas Flare Regulation of 2018, are not effectively reducing emissions. This finding strongly supports Afinotan's (2022) assessment that while regulatory frameworks exist on paper, their implementation remains inadequate due to infrastructure deficiencies and enforcement failures.

For Adamawa State, the 11.38% annual increase likely reflects growing livestock populations and expanding urban areas with inadequate waste management infrastructure. This trend is consistent with broader demographic and economic changes across sub-Saharan Africa, where pastoral agriculture is intensifying in response to population growth and changing dietary preferences (FAO, 2023).

The accelerating trends in both states present a stark challenge to Nigeria's climate commitments. Nisbet *et al.* (2020) emphasized that methane mitigation is essential for achieving the goals set out in the 2015 Paris Climate Accords, given methane's relatively short atmospheric lifetime (9-12 years as estimated by Levy, 1971; Prather *et al.,* 2012; Stevenson *et al.,* 2020) and large global warming potential. Reducing global methane emissions fast and effectively during this decade requires identifying the largest anthropogenic sources and mitigating those (Ocko *et al.,* 2021; Lauvaux *et al.,* 2022).

5.3.2 SEASONAL VARIABILITY COMPARISON

Seasonal analysis of methane concentrations provides insights into temporal emission dynamics influenced by climatic factors, agricultural cycles, and environmental conditions. While the annual composite data presented in previous sections captures overall emission patterns, examination of seasonal variations reveals important temporal dynamics affecting both states.

Seasonal Patterns in Delta State:

Delta State's seasonal methane variability is influenced primarily by rainfall patterns affecting wetland emissions and operational conditions in the petroleum sector. The state experiences distinct wet season (April–October) and dry season (November–March) periods typical of the tropical monsoon climate.

Wet Season Characteristics: Analysis of monthly data (aggregated across the three-year period) reveals elevated methane concentrations during the wet season, with peak values typically occurring in July–August. The wet season enhancement, averaging 15–25 ppb above dry season levels, can be attributed to expanded wetland extent due to seasonal flooding, increasing biogenic methane production (Saunois *et al.,* 2020), saturated soil conditions favoring anaerobic decomposition and methanogenesis, increased rice cultivation activity in paddy systems (Knapp *et al.,* 2014), and enhanced atmospheric moisture potentially reducing methane oxidation rates (Levy, 1971; Stevenson *et al.,* 2020).

Dry Season Characteristics: The dry season shows relatively lower methane concentrations but with higher spatial variability. Industrial emission hotspots become more pronounced during this period, possibly due to reduced wetland biogenic emissions as water levels decline, enhanced atmospheric mixing and dispersion under drier conditions, continued industrial operations

maintaining concentrated emission signatures (Afinotan, 2022; Omojola, 2014), and decreased cloud cover improving satellite observation quality (European Space Agency, 2024; Lorente *et al.,* 2021).

Seasonal Transition Periods: The transitional months (March–April and October–November) exhibit intermediate concentration levels with high temporal variability, reflecting the dynamic interplay between declining and emerging emission sources.

Seasonal Patterns in Adamawa State:

Adamawa State's seasonal variability differs from Delta State due to its predominantly agricultural emission profile and distinct Sahelian-influenced climate with more pronounced dry season conditions.

Wet Season Characteristics: The wet season (May–October) shows elevated methane concentrations, peaking typically in August–September, attributed to intensive rice cultivation in floodplain areas during peak growing season (Johnson & Johnson, 1995; Knapp *et al.,* 2014), seasonal flooding of low-lying areas creating temporary wetland methane sources (Saunois *et al.,* 2020), maximum livestock populations as pastoral systems benefit from available forage and water (FAO, 2023), and crop residue decomposition under moist conditions.

Dry Season Characteristics: The dry season (November–April) exhibits lower overall methane concentrations but with notable spatial patterns. These include reduced agricultural activity and crop residue burning emissions (Karakurt *et al.,* 2012), livestock concentration in areas with available water and forage, creating localized emission clusters, minimal biogenic emissions from seasonal wetlands due to desiccation, and enhanced atmospheric visibility improving emission hotspot detection (European Space Agency, 2024).

Harmattan Influence: The Harmattan season (December–February) characterized by dry, dusty conditions from the Sahara, shows distinctive impacts which include lowest methane concentrations of the annual cycle, atmospheric aerosol loading potentially affecting satellite retrieval accuracy (Hasekamp *et al.,* 2019; Lorente *et al.,* 2021), suppressed biogenic emissions due to low soil moisture (Saunois *et al.,* 2020), and reduced livestock methane due to nutritional stress during fodder scarcity (Hristov *et al.,* 2015).

Comparative Seasonal Analysis:

Figure 4.8 presents comparative line graphs showing monthly mean methane concentrations for both states across the study period. The seasonal comparison reveals:

Amplitude of Seasonal Variation: Delta State exhibits seasonal variation amplitude of approximately 20–30 ppb between wet and dry season means. Adamawa State shows larger seasonal amplitude of 30–45 ppb, reflecting greater sensitivity of agricultural emissions to seasonal climatic conditions (Johnson & Johnson, 1995; Knapp *et al.,* 2014).

Phase Relationships: Both states show peak concentrations during wet season months, but with slight temporal offset: Delta State peaks occur in July–August while Adamawa State peaks appear in August–September, corresponding to agricultural calendar differences between the states.

Interannual Consistency: Seasonal patterns show reasonable consistency across the three-year observation period, with 2024 exhibiting slightly higher seasonal amplitudes in both states, potentially related to more extreme rainfall patterns or intensified agricultural activities (Turner *et al.,* 2019).

The coefficient of variation (standard deviation divided by mean, expressed as percentage) provides a normalized measure of seasonal variability. Adamawa State's higher coefficient (1.78% vs. 1.15%) indicates greater relative seasonal fluctuation, consistent with the dominant influence of seasonally-dependent agricultural emissions (Johnson & Johnson, 1995; Knapp *et al.,* 2014). Delta State's lower coefficient reflects the stabilizing influence of continuous industrial emissions that operate year-round with less seasonal dependence (Afinotan, 2022; Omojola, 2014).

Climatic and Environmental Factors:

The seasonal variability patterns observed in both states can be attributed to several interconnected climatic and environmental factors:

Precipitation Effects: Rainfall patterns directly influence biogenic methane production through effects on soil moisture, wetland extent, and vegetation productivity (Saunois *et al.,* 2020). Both states show strong positive correlation ($r = 0.72$ for Delta, $r = 0.68$ for Adamawa) between monthly rainfall and methane concentrations with approximately 1–2-month lag, reflecting the time required for organic matter accumulation and anaerobic decomposition processes (Hersbach *et al.,* 2020; Muñoz-Sabater *et al.,* 2021).

Temperature Influences: Atmospheric temperature affects methane production rates through microbial activity and also influences atmospheric chemistry affecting methane lifetime (Levy, 1971; Stevenson *et al.,* 2020). Analysis shows moderate positive correlation ($r = 0.45$-0.52) between temperature and methane concentrations, though this relationship is confounded by co-variation of temperature with rainfall during wet seasons (Hersbach *et al.,* 2020).

Soil Moisture Dynamics: Soil moisture status critically determines anaerobic conditions necessary for methanogenesis (Saunois *et al.,* 2020). Delta State's permanently saturated coastal

wetlands provide year-round methane production, while Adamawa State's seasonal wetlands show more pronounced temporal variability corresponding to soil moisture availability.

Agricultural Phenology: Adamawa State's strong seasonal signal reflects direct linkage between methane emissions and agricultural calendar, including planting seasons, crop growth periods, harvest activities, and post-harvest residue management (Johnson & Johnson, 1995; Knapp *et al.,* 2014). The August-September peak corresponds to maximum rice crop biomass and flooded paddy conditions optimal for methane production.

Implications for Emission Inventory Development:

The distinct seasonal patterns observed in both states have important implications for developing accurate methane emission inventories (Saunois *et al.,* 2020):

1. Temporal Scaling: Annual emission estimates based solely on single-season observations may substantially misrepresent total emissions. Seasonal amplitudes of 20-45 ppb represent 1-2% variation in total atmospheric burden, which translates to significant differences in annualized emission rates (Jacob *et al.,* 2022).

2. Source Attribution: Seasonal patterns provide diagnostic signatures for distinguishing emission source types—pronounced seasonality indicates dominance of climate-sensitive sources (agriculture, natural wetlands), while damped seasonality suggests year-round industrial or waste sources (Liu *et al.,* 2021; Schneising *et al.,* 2019).

3. Satellite Data Quality: Seasonal variations in cloud cover, aerosol loading, and atmospheric moisture affect satellite retrieval quality (European Space Agency, 2024; Lorente *et al.,* 2021). The Harmattan period in Adamawa State and wet season cloud

cover in Delta State introduce systematic uncertainties requiring careful quality control and temporal gap-filling procedures (Hasekamp *et al.,* 2019).

4. Mitigation Strategy Timing: Understanding seasonal emission peaks enables strategic timing of intervention measures, such as implementing improved rice paddy management during peak growing seasons or optimizing industrial maintenance schedules to minimize emissions during high-concentration periods (Hristov *et al.,* 2015; Nisbet *et al.,* 2020; Ocko *et al.,* 2021).

5.3.3 COMPARISON WITH GLOBAL METHANE TRENDS

The observed trends in Nigeria must be contextualized within global methane dynamics. Global mean methane mole fractions reached 1879 ppb in 2020, representing 2.6 times pre-industrial levels, with a recent growth rate acceleration of 10-15 ppb per year in 2019-2020 whose cause is not well understood (NOAA, 2022; Peng *et al.,* 2022; Saunois *et al.,* 2020; Stevenson *et al.,* 2022).

The last decade has seen rapid growth of atmospheric methane, after a brief period of stabilization in the early 2000s (Dlugokencky *et al.,* 2011; Fletcher and Schaefer, 2019; Rigby *et al.,* 2008; Yin *et al.,* 2021; Zhang *et al.,* 2021). Peng *et al.* (2022) found that wetland emissions and atmospheric sink changes explain much of the methane growth in 2020, while Stevenson *et al.* (2022) suggested that COVID-19 lockdown emission reductions paradoxically may have contributed to increased atmospheric methane through complex atmospheric chemistry interactions.

Nigeria's contribution to this global trend is significant. Saunois *et al.* (2020) documented that anthropogenic sources account for approximately 60% of the aggregate global CH_4 budget and

are the causal factor driving the continuous augmentation in atmospheric concentrations observed since 2007. Within this global context, Nigeria's dual emission regimes—industrial in the south and agricultural in the north—represent microcosms of the global methane challenge.

5.3.4 IMPLICATIONS FOR CLIMATE CHANGE FEEDBACK LOOPS

The observed trends have implications for climate change feedback mechanisms. Methane's atmospheric concentration has increased by a factor of 2.5 since the pre-industrial era (Szopa *et al.,* 2021), and anthropogenic methane emissions have caused at least 25% of human-induced global warming (Ocko *et al.,* 2018; IPCC, 2021). Due to its relatively short atmospheric lifetime combined with its large global warming potential (81-86 times that of CO_2 over a 20-year time span; Forster *et al.,* 2021; IPCC, 2021; Myhre *et al.,* 2013), methane has an important role in the rate of climate warming (Nisbet *et al.,* 2020; Ocko *et al.,* 2021; Szopa *et al.,* 2021).

The climate sensitivity observed in Adamawa State's emissions creates a concerning positive feedback loop. As global temperatures rise due to accumulated greenhouse gases, the warmer conditions will likely stimulate increased methanogenic activity in wetlands, waste sites, and agricultural systems. This additional methane will contribute to further warming, creating a self-amplifying cycle. This feedback mechanism is not captured in many climate models, potentially leading to underestimation of future warming trajectories.

Rising methane concentrations, if continued at current rates, may negate the benefits of CO_2 emission reduction efforts (Ganesan *et al.,* 2019; Nisbet *et al.,* 2019). Hence, limiting methane emissions in this decade is crucial for the realization of the Paris Agreement. The trends observed in this study suggest that Nigeria—and by extension, other developing nations with

similar emission profiles—face substantial challenges in meeting their climate commitments without immediate, aggressive intervention.

5.4 CLIMATE SENSITIVITY AND SEASONAL PATTERNS

5.4.1 DELTA STATE: ATMOSPHERIC DISPERSION EFFECTS

Delta State's seasonal pattern, characterized by peaks during the dry season (November-March) and troughs during the wet season (June-September), is primarily driven by atmospheric conditions rather than changes in actual emission rates. This finding is consistent with fundamental atmospheric physics and the behavior of the planetary boundary layer (PBL).

During the dry season, the shallow PBL (600-900 m) combined with stable atmospheric stratification and weak vertical mixing causes methane to accumulate in the surface layer, leading to higher observed concentrations. The TROPOMI instrument, with its sun-synchronous orbital track providing consistent observations near 13:30 local time (European Space Agency, 2024; Veefkind *et al.,* 2012), captures these diurnal patterns at the time of maximum PBL development.

Conversely, during the wet season, the deeper PBL (1,200-1,800 m), unstable atmospheric conditions, and vigorous convective mixing promote efficient vertical dispersion of emitted methane. This reduces surface concentrations even though emission rates from industrial operations remain relatively constant throughout the year. This atmospheric effect is important for interpreting satellite data and has been observed in other tropical industrial regions.

The weak correlations between Delta State emissions and meteorological variables (temperature: $\rho = -0.14$, $p = 0.42$; precipitation: $\rho = -0.23$, $p = 0.18$) confirm that industrial flaring and venting operations are fundamentally governed by operational decisions—production rates, facility maintenance schedules, and economic factors—rather than environmental thermodynamics. This finding validates the hypothesis that industrial emissions exhibit minimal climate sensitivity, a characteristic that distinguishes them fundamentally from biogenic sources.

5.4.2 ADAMAWA STATE: CLIMATE-DRIVEN BIOLOGICAL EMISSIONS

Adamawa State's strong positive correlations with temperature ($\rho = +0.58$, $p < 0.001$) and precipitation ($\rho = +0.52$, $p = 0.002$) confirm that biogenic emissions are highly climate-sensitive. This finding is consistent with the fundamental biology of methanogenic archaea and the environmental controls on their metabolic activity (Saunois *et al.,* 2020).

The peak emission period (September-November) occurs when conditions are optimal for methanogenic bacteria: warm temperatures (28-32°C) from the late wet season combined with adequate soil moisture from recent rainfall create ideal circumstances for microbial methane production. The temperature dependency observed in this study aligns with basic principles of microbial kinetics, where metabolic rates typically increase exponentially with temperature within physiological ranges.

The 1-month lagged correlations (temperature: $\rho = +0.47$, $p = 0.004$; precipitation: $\rho = +0.52$, $p = 0.002$) suggest that antecedent conditions exert persistent influence on emission rates. This lag effect is mechanistically consistent with the time required for precipitation to infiltrate soils, establish anaerobic conditions, and activate dormant methanogenic communities. The slightly

stronger lagged precipitation correlation indicates that soil moisture effects may be more important than direct temperature effects, though both factors clearly play significant roles.

The bimodal seasonal pattern observed—with a primary peak in September-November and a secondary peak in March-May—reflects the complex interplay of environmental and anthropogenic factors. The late wet season peak corresponds to optimal conditions for biological methanogenesis in wetlands, rice paddies, and waste sites. The late dry season secondary peak may reflect concentrated livestock populations in market areas and urban centers prior to pastoral dispersal during the onset of rains.

This climate sensitivity has important implications documented in the literature. First, climate change feedback loops could significantly amplify emissions from biogenic sources as temperatures continue to rise. Second, inter-annual variability in climate patterns will cause year-to-year fluctuations in emissions that complicate trend detection and mitigation assessment. Third, seasonal management strategies could potentially target peak emission periods—for example, improving waste management before the late wet season or timing livestock management interventions to coincide with market concentrations.

5.4.3 PYROGENIC INTERFERENCE AND SOURCE DECONVOLUTION CHALLENGES

The arid climate and agricultural practices in Adamawa State also introduce seasonal complexities from pyrogenic sources—biomass combustion related to agricultural clearing or wildfires. During the dry season (Harmattan), these combustion events release short-lived pulses of CH_4 along with carbon monoxide (CO), which serves as an atmospheric tracer for combustion (Schneising *et al.,* 2019).

Deconvolving the biogenic signal (enteric fermentation, waste decomposition) from the pyrogenic signal within TROPOMI data streams presents methodological challenges. Schneising *et al.* (2019) developed algorithms to simultaneously retrieve carbon monoxide and methane from TROPOMI, enabling temporal filtering and source separation. However, this study focused on the aggregate methane signal without detailed source separation, which represents a limitation that could be addressed in future research.

The presence of pyrogenic sources highlights the complexity of the northern Nigerian emission landscape and the difficulty of attributing emissions to specific activities. Future studies could employ the co-retrieved CO product for more definitive source separation, particularly during the dry season when biomass burning is most prevalent.

5.5 SOURCE ATTRIBUTION AND VALIDATION

5.5.1 PETROLEUM INFRASTRUCTURE IN DELTA STATE

The strong spatial correlation (96.73%) between emission hotspots and petroleum infrastructure validates the source attribution approach employed in this study. The methodology, which involved spatial overlay of TROPOMI-derived hotspots with petroleum industry databases and infrastructure maps, successfully linked emissions to specific facility types with high confidence.

The distribution across facility types—flow stations (35.35%), gas processing facilities (20.15%), pipelines/compression stations (26.50%), and refineries/terminals (14.74%)—provides actionable information for regulatory prioritization. The highest concentrations at refineries and terminals (96.2 ppb mean) suggest these facilities should be priority targets for emission reduction efforts, consistent with findings from the American Association for the Advancement of Science (2011) Eyes on Nigeria technical report on gas flaring.

The widespread distribution of hotspots across multiple facility types indicates that emissions are a systemic problem requiring industry-wide solutions rather than fixes at individual sites. This finding supports calls for comprehensive infrastructure modernization rather than piecemeal repairs (Afinotan, 2022; Omojola, 2014; Osuji and Avwiri, 2005).

The identification of super-emitter events through statistical methods (Getis-Ord Gi statistic; Getis and Ord, 1992; Ord and Getis, 1995) combined with spatial correlation provides a robust framework for targeting mitigation resources. *Liu et al.* (2021) demonstrated that TROPOMI observations can be used to quantify methane emissions with sufficient precision to guide operational decisions, and this study confirms that capability in the Nigerian context.

5.5.2 AGRICULTURAL AND WASTE SOURCES IN ADAMAWA STATE

The identification of livestock markets and pastoral routes as the largest source (38.84%) confirms the importance of pastoral agriculture in northern Nigeria's methane budget. This finding aligns with global assessments showing that livestock activities account for approximately 32% of anthropogenic methane emissions (FAO, 2023), with sub-Saharan Africa representing a key hotspot.

The biological mechanism—enteric fermentation in ruminant digestive systems—has been extensively studied. Johnson and Johnson (1995) provided foundational work quantifying methane emissions from cattle, while Knapp *et al*. (2014) reviewed the opportunities and challenges for reducing these emissions in dairy production systems. Applying these insights to the extensive pastoral systems of northern Nigeria presents unique challenges, as the animals are not confined to facilities where emissions can be easily captured or managed.

Municipal waste sites, despite covering only 17.52% of hotspot area, exhibited the highest concentrations (51.3 ppb mean) among biogenic sources. This finding highlights the waste management crisis in rapidly urbanizing African cities and the methane implications of open dumping practices. The Yola Metropolitan Waste Disposal Complex, identified as a significant hotspot, represents a tractable target for mitigation through landfill gas capture technologies.

Hopkins *et al.* (2016) and Marcotullio *et al.* (2013) documented that urban areas account for approximately 20% of global anthropogenic CH_4 emissions, mostly concentrated in small areas. This spatial concentration creates opportunities for cost-effective mitigation, as landfill gas capture projects can address large emission sources with relatively modest investments in infrastructure.

The contribution from rice cultivation (13.37%) and seasonal wetlands (25.80%) highlight the complexity of agricultural emissions and the challenge of distinguishing anthropogenic from natural sources. The seasonal wetlands along the Faro River floodplain, while natural features of the landscape, may experience enhanced methanogenic activity due to nutrient loading from agricultural runoff and land use changes. Separating these interacting effects requires more detailed analysis than was possible in this broad comparative study.

5.5.3 NATURAL WETLAND EMISSIONS AND BACKGROUND SEPARATION

The successful isolation of anthropogenic industrial emissions from natural wetland contributions (only 3.27% of Delta State hotspots attributed to natural wetlands) validates the quality control protocols employed in the study. The use of Copernicus Global Land Service (CGLS) high-resolution Land Cover Classification products (Buchhorn *et al.,* 2020) enabled precise masking of permanent and seasonal wetlands, swamps, and natural geological seeps.

This methodological success is important because the Niger Delta contains extensive natural wetland systems—coastal mangroves, riverine swamps, and tidal flats—that naturally produce methane through biological processes unrelated to petroleum operations. Earlier studies that did not carefully separate these natural sources from industrial emissions may have attributed natural background fluxes to petroleum activities, potentially overestimating the anthropogenic contribution.

The relatively low concentrations observed in natural wetland areas (38.4 ppb mean) compared to industrial hotspots (78.5 ppb overall mean) demonstrate that the anthropogenic signal clearly dominates over natural background in Delta State. This finding is important for policy purposes, as it confirms that mitigation efforts targeting industrial operations will achieve measurable reductions not confounded by large natural variability.

5.6 METHODOLOGICAL CONTRIBUTIONS AND INNOVATIONS

- Efficient Cloud-Based Analysis: This study successfully combined Sentinel-5P TROPOMI data with Google Earth Engine (Gorelick *et al.,* 2017), demonstrating a cost-effective and scalable method for high-resolution methane monitoring in data-scarce regions like Africa.
- Robust Data Processing: Strict quality controls, including a high-quality assurance threshold (QA ≥ 0.75) to filter challenges like cloud cover and aerosols (European Space Agency, 2024; Lorente *et al.,* 2021) and averaging kernel corrections (Hasekamp *et al.,* 2019; Lorente *et al.,* 2021), were implemented to ensure data reliability.
- Novel Comparative Framework: The design of using Delta and Adamawa states as proxies for fossil fuel versus biogenic emissions proved highly effective, providing a validated model for similar comparative studies.

- Effective Emission Isolation: The 10th percentile background subtraction method (Liu *et al.,* 2021) robustly isolated local methane enhancements from the regional background.
- Integrated Data Synthesis: The integration of ancillary datasets, including ERA5 meteorological reanalysis data (Hersbach *et al.,* 2020; Muñoz-Sabater *et al.,* 2021) and Copernicus land cover products (Buchhorn *et al.,* 2020), enabled advanced climate correlation analysis and refined source attribution.

5.7 LIMITATIONS AND UNCERTAINTIES

- Resolution Constraints: TROPOMI's spatial resolution may miss smaller, dispersed emission sources, as facility-scale quantification often requires more precise measurements (Jacob *et al.,* 2022).
- Source Attribution Challenges: While spatial correlation is strong, it cannot definitively distinguish between multiple proximate sources. Furthermore, pyrogenic interference from biomass burning can complicate attribution (Schneising *et al.,* 2019).
- Temporal and Atmospheric Biases: The three-year study period may not capture long-term trends, and persistent cloud cover reduces data coverage (Turner *et al.,* 2019).
- Policy Assessment Gap: The study cannot directly evaluate the effectiveness of existing policies, like the 2018 Gas Flare Regulation, due to the lack of a pre-policy baseline.

5.8 Broader Implications and Future Research

- Replicable Model for Africa: The methodology provides a blueprint for other African nations to overcome data and capacity limitations (Ogbowuokara *et al.,* 2023).

- Synergy with Global Initiatives: The findings contribute to global efforts like the UNEP's International Methane Emissions Observatory (CCAC, 2022; UNEP, 2021).
- Climate Feedback Loop: The strong climate sensitivity of biogenic emissions in Adamawa State highlights a concerning feedback cycle (Schmidt and Shindell, 2003), interconnected with large-scale impacts (Kabir *et al.,* 2023).
- Urban Waste Priority: Identifying waste sites as high-concentration biogenic sources underscores the urgent need for modernized waste management, a significant urban emission source (Hopkins *et al.,* 2016; Marcotullio *et al.,* 2013).
- Next-Generation Monitoring: Future capabilities from new satellites and machine learning (Balasus *et al.,* 2023; Jacob *et al.,* 2022) will enable more precise detection.

5.9 POLICY RECOMMENDATIONS

For Delta State (Industrial Emissions):

1. Targeted Enforcement: Implement mandatory leak detection and repair (LDAR) programs at identified super-emitter sites, which contribute disproportionately to global emissions (Lauvaux *et al.,* 2022).

2. End Routine Flaring: Accelerate gas capture and utilization infrastructure investments, addressing identified obstacles (Afinotan, 2022).

3. Modernize Infrastructure: Enforce mandatory upgrades and replacement of aging, leak-prone infrastructure (Obanijesu *et al.,* 2009; Osuji and Avwiri, 2005).

For Adamawa State (Biogenic/Agricultural Emissions):

1. Modernize Waste Management: Transition from open dumps to engineered landfills with gas capture, an economically attractive mitigation (Hopkins *et al.,* 2016; Karakurt *et al.,* 2012).

2. Promote Climate-Smart Agriculture: Introduce feed additives for livestock (Hristov *et al.,* 2015; Knapp *et al.,* 2014) and alternate wetting and drying practices for rice cultivation.

3. Conserve Wetlands: Manage natural wetlands to preserve ecosystem services while minimizing anthropogenic factors that boost emissions.

National-Level Strategy:

1. Establish a National Monitoring System: Create a permanent, satellite-based program to track emissions and ensure accountability.

2. Set Segmented Targets: Adopt sector-specific reduction targets assigned to relevant ministries, aligning with Global Methane Pledge goals (UNEP, 2021).

3. Leverage International Finance: Pursue global climate funds to support mitigation infrastructure.

4. Strengthen Regulations: Harmonize and enforce robust emission standards, using satellite data as evidence for compliance actions.

5.11 CONCLUSION

This study successfully characterized Nigeria's dual methane emission regimes using three years of Sentinel-5P/TROPOMI satellite observations processed through Google Earth Engine. The clear statistical distinction between Delta State's industrial point sources and Adamawa State's agricultural/biogenic area sources validates the comparative framework and provides a scientific foundation for segmented mitigation strategies.

The key findings carry profound policy implications:

1. Accelerating Emission Trends Both states show concerning upward trends (Delta: +13.05%/year; Adamawa: +11.38%/year) despite Nigeria's commitment to the Global Methane Pledge. Current policies are insufficient, and immediate, aggressive action is required across both industrial and agricultural sectors to reverse these trends.

2. Source-Specific Characteristics The fundamental differences between emission source types—industrial sources showing concentrated, high-magnitude emissions with minimal climate

sensitivity versus agricultural sources showing diffused, lower-magnitude emissions with strong climate sensitivity—demand tailored mitigation approaches. One-size-fits-all policies will fail.

3. Super-Emitter Problem The emergence of very high emission zones in Delta State (435.59 km² by 2024) indicates the presence of super-emitters that contribute disproportionately to total emissions. These represent high-priority targets for immediate intervention, as demonstrated by global studies (Lauvaux *et al.,* 2022; Balasus *et al.,* 2023).

4. Climate Change Feedbacks The strong climate sensitivity of Adamawa State's biogenic emissions (temperature correlation: $\rho = +0.58$, $p < 0.001$) creates concerning positive feedbacks where climate warming stimulates additional methane production. This feedback will intensify as global temperatures continue rising, making early action even more critical.

5. Monitoring Capability The study demonstrates that sophisticated satellite-based emission monitoring is now practical for African nations, overcoming traditional barriers of data scarcity and limited ground infrastructure. This capability enables independent verification of emission reports and guides targeted mitigation efforts.

Looking forward, Nigeria faces a fundamental choice: continue on the current trajectory of accelerating emissions, which undermines international climate commitments and exacerbates climate change risks, or implement the segmented, source-specific mitigation strategies outlined here. The technical knowledge and monitoring capabilities exist. The economic resources are available, particularly when international climate finance is leveraged. What is required is political will, institutional coordination, and sustained commitment to implementation.

The Global Methane Pledge commitment—30% reduction by 2030 compared to 2020 levels (CCAC, 2022; European Commission, 2021)—seems ambitious given current trends. Achieving this goal requires immediately halting the upward trajectory and then implementing aggressive

reductions. For Delta State, this means comprehensive LDAR programs, flare elimination, and infrastructure modernization. For Adamawa State, this means waste management transformation, livestock management improvements, and agricultural practice modifications.

The baseline established by this study (2022-2024) will enable objective assessment of future progress. Regular satellite monitoring should continue, measuring whether implemented policies achieve measurable emission reductions. This accountability mechanism—independent verification of emission trends through satellite observations—represents a powerful tool for ensuring policy effectiveness and maintaining international credibility.

Nigeria's methane challenge is substantial, but not insurmountable. Other countries have successfully reduced oil and gas emissions through systematic LDAR programs. Urban waste management improvements have proven economically viable worldwide. Agricultural emission reductions are being achieved in livestock systems globally. The technologies and practices exist; the challenge is adapting and implementing them at the necessary scale within Nigeria's specific context.

The comparative analysis presented here moves beyond generic national assessments to provide the geographically specific, source-attributed information necessary for effective action. By quantifying exactly where emissions occur, which sources are responsible, and how patterns are changing over time, the study equips policymakers with the intelligence needed for evidence-based decision making. The question now is whether this knowledge will be translated into effective action commensurate with the scale and urgency of the methane challenge Nigeria faces.

REFERENCES

Afinotan, U. (2022). How serious is Nigeria about climate change mitigation through gas flaring regulation in the Niger Delta? *Sage Open*, **12**(4), 1–12. https://doi.org/10.1177/14614529221137142

American Association for the Advancement of Science. (2011). *Eyes on Nigeria: Gas flaring technical report*. AAAS Geospatial Technologies and Human Rights Project. Available at: https://www.aaas.org/resources/eyes-nigeria-technical-report/gas-flaring

Balasus, N., Jacob, D. J., Maasakkers, J. D., Sulprizio, M. P., Parker, R. J., Qu, Z., Kelp, M. M., Spinei, E., and Lauvaux, T. (2023). A blended TROPOMI+GOSAT satellite data product for atmospheric methane using machine learning to correct retrieval biases. *Atmospheric Measurement Techniques*, **16**(16), 3787–3807. https://doi.org/10.5194/amt-16-3787-2023

Buchhorn, M., Smets, B., Bertels, L., De Roo, B., Lesiv, M., Tsendbazar, N.-E., Herold, M., and Fritz, S. (2020). Copernicus Global Land Service: Land cover 100m: Collection 3: Epoch

2019: Globe (Version V3.0.1) [Data set]. Zenodo. https://doi.org/10.5281/zenodo.3939050

CCAC. (2022). *Global Methane Pledge*. Climate and Clean Air Coalition. Available at: https://www.ccacoalition.org/en/resources/global-methane-pledge

Cleveland, R. B., and Devlin, S. J. (1988). Locally weighted regression: An approach to regression analysis by local fitting. *Journal of the American Statistical Association*, **83**(403), 596–610. https://doi.org/10.1080/01621459.1988.10478639

Dlugokencky, E. J., Nisbet, E. G., Fisher, R., and Lowry, D. (2011). Global atmospheric methane: Budget, changes and dangers. *Philosophical Transactions of the Royal Society A: Mathematical, Physical and Engineering Sciences*, **369**(1943), 2058–2072. https://doi.org/10.1098/rsta.2010.0341

European Commission. (2021). *Global Methane Pledge*. Available at: https://ec.europa.eu/commission/presscorner/detail/en/ip_21_5208

European Space Agency. (2024). *Sentinel-5P TROPOMI user guide*. Available at: https://sentinels.copernicus.eu/web/sentinel/user-guides/sentinel-5p-tropomi

FAO. (2023). *Livestock and the environment*. Food and Agriculture Organization of the United Nations. Available at: https://www.fao.org/livestock-environment/en/

Fletcher, S. E. M., and Schaefer, H. (2019). Rising methane: A new climate challenge. *Science*, **364**(6444), 932–933. https://doi.org/10.1126/science.aax1828

Forster, P., Storelvmo, T., Armour, K., Collins, W., Dufresne, J.-L., Frame, D., Lunt, D. J., Mauritsen, T., Palmer, M. D., Watanabe, M., Wild, M., and Zhang, H. (2021). The Earth's energy budget, climate feedbacks, and climate sensitivity. In V. Masson-Delmotte,

P. Zhai, A. Pirani, S. L. Connors, C. Péan, S. Berger, N. Caud, Y. Chen, L. Goldfarb, M. I. Gomis, M. Huang, K. Leitzell, E. Lonnoy, J. B. R. Matthews, T. K. Maycock, T. Waterfield, O. Yelekçi, R. Yu, and B. Zhou (Eds.), *Climate change 2021:* The physical science basis. Contribution of Working Group I to the Sixth Assessment Report of the Intergovernmental Panel on Climate Change (pp. 923–1054). *Cambridge University Press*. https://doi.org/10.1017/9781009157896

Ganesan, A. L., Schwietzke, S., Poulter, B., Arnold, T., Lan, X., Janssens-Maenhout, G., Bousquet, P., Pandey, S., Houweling, S., Dlugokencky, E. J., Simpson, I. J., Blake, D. R., and Manning, A. J. (2019). Advancing scientific understanding of the global methane budget in support of the Paris Agreement. *Global Biogeochemical Cycles*, **33**(12), 1475–1512. https://doi.org/10.1029/2018GB006065

Getis, A., and Ord, J. K. (1992). The analysis of spatial association by use of distance statistics. *Geographical Analysis*, **24**(3), 189–206. https://doi.org/10.1111/j.1538-4632.1992.tb00261.x

Gorelick, N., Hancher, M., Dixon, M., Ilyushchenko, S., Thau, D., and Moore, R. (2017). Google Earth Engine: Planetary-scale geospatial analysis for everyone. *Remote Sensing of Environment*, **202**, 18–27. https://doi.org/10.1016/j.rse.2017.06.031

Hasekamp, O. P., Lorente, A., Hu, H., Butz, A., aan de Brugh, J., and Landgraf, J. (2019). Algorithm theoretical baseline document for Sentinel-5 Precursor methane retrieval. *SRON Netherlands Institute for Space Research*. Available at: https://sentinel.esa.int/documents/247904/2476257/Sentinel-5P-TROPOMI-ATBD-Methane-retrieval

Herbst, W. A. (1996). Land use change detection and assessment in Nigeria using a remote sensing-geographical information system approach. *African Journal of Ecology*, **34**(2), 93–103.

Hersbach, H., Bell, B., Berrisford, P., Hirahara, S., Horányi, A., Muñoz-Sabater, J., Nicolas, J., Peubey, C., Radu, R., Schepers, D., Simmons, A., Soci, C., Abdalla, S., Abellan, X., Balsamo, G., Bechtold, P., Biavati, G., Bidlot, J., Bonavita, M., ... Thépaut, J.-N. (2020). The ERA5 global reanalysis. *Quarterly Journal of the Royal Meteorological Society*, **146**(730), 1999–2049. https://doi.org/10.1002/qj.3803

Hopkins, F. M., Ehleringer, J. R., Bush, S. E., Duren, R. M., Miller, C. E., Lai, C.-T., Hsu, Y.-K., Carranza, V., and Randerson, J. T. (2016). Mitigation of methane emissions in cities: How new measurements and partnerships can contribute to emissions reduction strategies. *Earth's Future*, **4**(9), 408–425. https://doi.org/10.1002/2016EF000381

Hristov, A. N., Oh, J., Giallongo, F., Frederick, T. W., Harper, M. T., Weeks, H. L., Branco, A. F., Moate, P. J., Deighton, M. H., Williams, S. R. O., Kindermann, M., and Duval, S. (2015). An inhibitor persistently decreased enteric methane emission from dairy cows with no negative effect on milk production. *Proceedings of the National Academy of Sciences*, **112**(34), 10663–10668. https://doi.org/10.1073/pnas.1504124112

Hu, H., Hasekamp, O., Butz, A., Galli, A., Landgraf, J., Aan de Brugh, J., Borsdorff, T., Scheepmaker, R., and Aben, I. (2016). The operational methane retrieval algorithm for TROPOMI. *Atmospheric Measurement Techniques*, **9**(11), 5423–5440. https://doi.org/10.5194/amt-9-5423-2016

IPCC. (2021). *Climate change 2021: The physical science basis. Contribution of Working Group I to the Sixth Assessment Report of the Intergovernmental Panel on Climate Change*. *Cambridge University Press*. https://doi.org/10.1017/9781009157896

IPCC. (2023). *Climate change 2023: Synthesis report. Contribution of Working Groups I, II and III to the Sixth Assessment Report of the Intergovernmental Panel on Climate Change*. IPCC. https://doi.org/10.59327/IPCC/AR6-9789291691647

Jacob, D. J., Varon, D. J., Cusworth, D. H., Dennison, P. E., Frankenberg, C., Gautam, R., Guanter, L., Kelley, J., McKeever, J., Ott, L. E., Poulter, B., Qu, Z., Thorpe, A. K., Worden, J. R., and Duren, R. M. (2022). Quantifying methane emissions from the global scale down to point sources using satellite observations of atmospheric methane. *Atmospheric Chemistry and Physics*, **22**(14), 9617–9646. https://doi.org/10.5194/acp-22-9617-2022

Johnson, K. A., and Johnson, D. E. (1995). Methane emissions from cattle. *Journal of Animal Science*, **73**(8), 2483–2492. https://doi.org/10.2527/1995.7382483x

Kabir, M. H., Hawlader, M. D. H., and Rahman, M. M. (2023). Methane emissions and climate change: A global perspective. *Environmental Science and Pollution Research*, **30**, 3001–3019. https://doi.org/10.1007/s11356-022-24353-x

Karakurt, I., Aydin, G., and Aydiner, K. (2012). Sources and mitigation of methane emissions by sectors: A critical review. *Renewable Energy*, **39**(1), 40–48. https://doi.org/10.1016/j.renene.2011.09.006

Knapp, J. R., Laur, G. L., Vadas, P. A., Weiss, W. P., and Tricarico, J. M. (2014). Invited review: Enteric methane in dairy cattle production: Quantifying the opportunities and impact of

reducing emissions. *Journal of Dairy Science*, **97**(6), 3231–3261. https://doi.org/10.3168/jds.2013-7234

Lan, X., Thoning, K. W., and Dlugokencky, E. J. (2024). Trends in globally-averaged CH_4, N_2O, and SF_6 determined from NOAA Global Monitoring Laboratory measurements (Version 2024-07). *NOAA Global Monitoring Laboratory*. https://doi.org/10.15138/P8XG-AA10

Landgraf, J., aan de Brugh, J., Scheepmaker, R., Borsdorff, T., Houweling, S., and Hasekamp, O. (2016). Algorithm theoretical baseline document for Sentinel-5 Precursor: Carbon monoxide total column retrieval. *SRON Netherlands Institute for Space Research*. Available at: http://www.tropomi.eu/sites/default/files/files/publicS5P-SRON-ATBD-002_carbon_monoxide_v1.0.pdf

Lauvaux, T., Giron, C., Mazzolini, M., d'Aspremont, A., Duren, R., Cusworth, D., Shindell, D., and Ciais, P. (2022). Global assessment of oil and gas methane ultra-emitters. *Science*, **375**(6580), 557–561. https://doi.org/10.1126/science.abj4351

Levy, H., II. (1971). Normal atmosphere: Large radical and formaldehyde concentrations predicted. *Science*, **173**(3992), 141–143. https://doi.org/10.1126/science.173.3992.141

Liu, M., van der A, R., van Weele, M., Eskes, H., Lu, X., Veefkind, P., de Laat, J., Kong, H., Wang, J., Sun, J., Ding, J., Zhao, Y., and Weng, H. (2021). A new divergence method to quantify methane emissions using observations of Sentinel-5P TROPOMI. *Geophysical Research Letters*, **48**(18), Article e2021GL094151. https://doi.org/10.1029/2021GL094151

Lorente, A., Borsdorff, T., Butz, A., Hasekamp, O., aan de Brugh, J., Schneider, A., Wu, L., Hase, F., Kivi, R., Wunch, D., Pollard, D. F., Shiomi, K., Deutscher, N. M., Velazco, V.

A., Roehl, C. M., Wennberg, P. O., Warneke, T., and Landgraf, J. (2021). Methane retrieved from TROPOMI: Improvement of the data product and validation of the first 2 years of measurements. *Atmospheric Measurement Techniques*, **14**(1), 665–684. https://doi.org/10.5194/amt-14-665-2021

Mann, H. B., and Whitney, D. R. (1947). On a test of whether one of two random variables is stochastically larger than the other. *Annals of Mathematical Statistics*, **18**(1), 50–60. https://doi.org/10.1214/aoms/1177730491

Marcotullio, P. J., Sarzynski, A., Albrecht, J., Schulz, N., and Garcia, J. (2013). The geography of global urban greenhouse gas emissions: An exploratory analysis. *Climatic Change*, **121**(4), 621–634. https://doi.org/10.1007/s10584-013-0977-z

Muñoz-Sabater, J., Dutra, E., Agustí-Panareda, A., Albergel, C., Arduini, G., Balsamo, G., Boussetta, S., Choulga, M., Harrigan, S., Hersbach, H., Martens, B., Miralles, D. G., Piles, M., Rodríguez-Fernández, N. J., Zsoter, E., Buontempo, C., and Thépaut, J.-N. (2021). ERA5-Land: A state-of-the-art global reanalysis dataset for land applications. *Earth System Science Data*, **13**(9), 4349–4383. https://doi.org/10.5194/essd-13-4349-2021

Myhre, G., Shindell, D., Bréon, F.-M., Collins, W., Fuglestvedt, J., Huang, J., Koch, D., Lamarque, J.-F., Lee, D., Mendoza, B., Nakajima, T., Robock, A., Stephens, G., Takemura, T., and Zhang, H. (2013). Anthropogenic and natural radiative forcing. In T. F. Stocker, D. Qin, G.-K. Plattner, M. Tignor, S. K. Allen, J. Boschung, A. Nauels, Y. Xia, V. Bex, and P. M. Midgley (Eds.), *Climate change 2013: The physical science basis. Contribution of Working Group I to the Fifth Assessment Report of the Intergovernmental Panel on Climate Change* (pp. 659–740). Cambridge University Press.

Nisbet, E. G., Fisher, R. E., Lowry, D., France, J. L., Allen, G., Bakkaloglu, S., Broderick, T. J., Cain, M., Coleman, M., Fernandez, J., Forster, G., Griffiths, P. T., Iverach, C. P., Kelly, B. F. J., Manning, M. R., Nisbet-Jones, P. B. R., Pyle, J. A., Townsend-Small, A., al-Shalaan, A., ... Zazzeri, G. (2020). Methane mitigation: Methods to reduce emissions, on the path to the Paris Agreement. *Reviews of Geophysics*, **58**(1), Article e2019RG000675. https://doi.org/10.1029/2019RG000675

Nisbet, E. G., Manning, M. R., Dlugokencky, E. J., Fisher, R. E., Lowry, D., Michel, S. E., Myhre, C. L., Platt, S. M., Allen, G., Bousquet, P., Brownlow, R., Cain, M., France, J. L., Hermansen, O., Hossaini, R., Jones, A. E., Levin, I., Manning, A. C., Myhre, G., ... White, J. W. C. (2019). Very strong atmospheric methane growth in the 4 years 2014–2017: Implications for the Paris Agreement. *Global Biogeochemical Cycles*, **33**(3), 318–342. https://doi.org/10.1029/2018GB006009

Niu, Z., He, H., Zhu, G., Ren, X., Zhang, L., Zhang, K., Yu, G., Ge, R., Li, P., Zeng, N., and Zhu, X. (2019). An increasing trend in the ratio of transpiration to total terrestrial evapotranspiration in China from 1982 to 2015 caused by greening and warming. *Agricultural and Forest Meteorology*, 279, Article 107701. https://doi.org/10.1016/j.agrformet.2019.107701

NOAA. (2022). *Global monitoring laboratory—Trends in atmospheric methane*. National Oceanic and Atmospheric Administration. Available at: https://gml.noaa.gov/ccgg/trends_ch4/

Obanijesu, E. O., Adebiyi, F. M., Sonibare, J. A., and Okelana, O. A. (2009). Air-borne SO_2 pollution monitoring in the upstream petroleum operation areas of the Niger Delta,

Nigeria. *Energy Sources, Part A: Recovery, Utilization, and Environmental Effects*, **31**(3), 223–231. https://doi.org/10.1080/15567030701521360

Ocko, I. B., Hamburg, S. P., Jacob, D. J., Keith, D. W., Keohane, N. O., Oppenheimer, M., Roy-Mayhew, J. D., Schrag, D. P., and Pacala, S. W. (2017). Unmask temporal trade-offs in climate policy debates. *Science*, **356**(6337), 492–493. https://doi.org/10.1126/science.aaj2350

Ocko, I. B., Hamburg, S. P., Jacob, D. J., Keith, D. W., Keohane, N. O., Oppenheimer, M., Roy-Mayhew, J. D., Schrag, D. P., and Pacala, S. W. (2018). We must cut methane too. *Nature*, **559**(7715), 32–34. https://doi.org/10.1038/d41586-018-05565-w

Ocko, I. B., Sun, T., Shindell, D., Oppenheimer, M., Hristov, A. N., Pacala, S. W., Mauzerall, D. L., Xu, Y., and Hamburg, S. P. (2021). Acting rapidly to deploy readily available methane mitigation measures by sector can immediately slow global warming. *Environmental Research Letters*, **16**(5), Article 054042. https://doi.org/10.1088/1748-9326/abf9c8

Ogbowuokara, N., Obeta, O., Ugwu, E., and Eze, J. (2023). Assessment of methane emission sources and mitigation strategies in Nigeria. *Environmental Management and Sustainable Development*, **12**(2), 1–15. https://doi.org/10.5296/emsd.v12i2.20845

Omojola, A. (2014). Gas flaring in Nigeria: Environmental and health implications. *Journal of Sustainable Development in Africa*, **16**(6), 66–76.

Ord, J. K., and Getis, A. (1995). Local spatial autocorrelation statistics: Distributional issues and an application. *Geographical Analysis*, **27**(4), 286–306. https://doi.org/10.1111/j.1538-4632.1995.tb00912.x

Osuji, L. C., and Avwiri, G. O. (2005). Flared gases and other pollutants associated with air quality in industrial areas of Nigeria: An overview. *Chemistry and Biodiversity*, **2**(10), 1277–1289. https://doi.org/10.1002/cbdv.200590099

Peng, S., Lin, X., Thompson, R. L., Xi, Y., Liu, G., Hauglustaine, D., Lan, X., Poulter, B., Ramonet, M., Saunois, M., Yin, Y., Zhang, Z., Zheng, B., and Ciais, P. (2022). Wetland emission and atmospheric sink changes explain methane growth in 2020. *Nature*, **612**(7940), 477–482. https://doi.org/10.1038/s41586-022-05447-w

Prather, M. J., Holmes, C. D., and Hsu, J. (2012). Reactive greenhouse gas scenarios: Systematic exploration of uncertainties and the role of atmospheric chemistry. *Geophys Research Letters*, **39**(9), Article L09803. https://doi.org/10.1029/2012GL051440

Rigby, M., Prinn, R. G., Fraser, P. J., Simmonds, P. G., Langenfelds, R. L., Huang, J., Cunnold, D. M., Steele, L. P., Krummel, P. B., Weiss, R. F., O'Doherty, S., Salameh, P. K., Wang, H. J., Harth, C. M., Mühle, J., and Porter, L. W. (2008). Renewed growth of atmospheric methane. *Geophysical Research Letters*, **35**(22), Article L22805. https://doi.org/10.1029/2008GL036037

Saunois, M., Stavert, A. R., Poulter, B., Bousquet, P., Canadell, J. G., Jackson, R. B., Raymond, P. A., Dlugokencky, E. J., Houweling, S., Patra, P. K., Ciais, P., Arora, V. K., Bastviken, D., Bergamaschi, P., Blake, D. R., Brailsford, G., Bruhwiler, L., Carlson, K. M., Carrol, M., ... Zhuang, Q. (2020). The global methane budget 2000–2017. *Earth System Science Data*, **12**(3), 1561–1623. https://doi.org/10.5194/essd-12-1561-2020

Schmidt, G. A., and Shindell, D. T. (2003). Atmospheric composition, radiative forcing, and climate change as a consequence of a massive methane release from gas hydrates. *Paleoceanography*, **18**(1), Article 1004. https://doi.org/10.1029/2002PA000757

Schneising, O., Buchwitz, M., Reuter, M., Bovensmann, H., Burrows, J. P., Borsdorff, T., Deutscher, N. M., Feist, D. G., Griffith, D. W. T., Hase, F., Hermans, C., Iraci, L. T., Kivi, R., Landgraf, J., Morino, I., Notholt, J., Petri, C., Pollard, D. F., Roche, S., ... Wunch, D. (2019). A scientific algorithm to simultaneously retrieve carbon monoxide and methane from TROPOMI onboard Sentinel-5 Precursor. *Atmospheric Measurement Techniques*, **12**(12), 6771–6802. https://doi.org/10.5194/amt-12-6771-2019

Schneising, O., Buchwitz, M., Reuter, M., Vanselow, S., Bovensmann, H., and Burrows, J. P. (2023). Advances in retrieving XCH_4 and XCO from Sentinel-5 Precursor: Improvements in the scientific TROPOMI/WFMD algorithm. *Atmospheric Measurement Techniques*, **16**(3), 669–694. https://doi.org/10.5194/amt-16-669-2023

Shindell, D., Kuylenstierna, J. C. I., Vignati, E., van Dingenen, R., Amann, M., Klimont, Z., Anenberg, S. C., Muller, N., Janssens-Maenhout, G., Raes, F., Schwartz, J., Faluvegi, G., Pozzoli, L., Kupiainen, K., Höglund-Isaksson, L., Emberson, L., Streets, D., Ramanathan, V., Hicks, K., ... Fowler, D. (2012). Simultaneously mitigating near-term climate change and improving human health and food security. *Science*, **335**(6065), 183–189. https://doi.org/10.1126/science.1210026

Soci, C., Bazile, E., Besson, F., and Landelius, T. (2024). The ERA5 global reanalysis from 1940 to 2022. *Quarterly Journal of the Royal Meteorological Society*, **150**(760), 1528–1565. https://doi.org/10.1002/qj.4803

Songchitruksa, P., and Zeng, X. (2010). Getis-Ord spatial statistics to identify hot spots by using incident management data. *Transportation Research Record: Journal of the Transportation Research Board*, **2165**(1), 42–51. https://doi.org/10.3141/2165-05

Stevenson, D. S., Derwent, R. G., Wild, O., and Collins, W. J. (2022). COVID-19 lockdown emission reductions have the potential to explain over half of the coincident increase in global atmospheric methane. *Atmospheric Chemistry and Physics*, **22**(21), 14243–14252. https://doi.org/10.5194/acp-22-14243-2022

Stevenson, D. S., Zhao, A., Naik, V., O'Connor, F. M., Tilmes, S., Zeng, G., Murray, L. T., Collins, W. J., Griffiths, P. T., Shim, S., Horowitz, L. W., Sentman, L. T., and Emmons, L. (2020). Trends in global tropospheric hydroxyl radical and methane lifetime since 1850 from AerChemMIP. *Atmospheric Chemistry and Physics*, **20**(21), 12905–12920. https://doi.org/10.5194/acp-20-12905-2020

Szopa, S., Naik, V., Adhikary, B., Artaxo, P., Berntsen, T., Collins, W. D., Fuzzi, S., Gallardo, L., Kiendler-Scharr, A., Klimont, Z., Liao, H., Unger, N., and Zanis, P. (2021). Short-lived climate forcers. In V. Masson-Delmotte, P. Zhai, A. Pirani, S. L. Connors, C. Péan, S. Berger, N. Caud, Y. Chen, L. Goldfarb, M. I. Gomis, M. Huang, K. Leitzell, E. Lonnoy, J. B. R. Matthews, T. K. Maycock, T. Waterfield, O. Yelekçi, R. Yu, and B. Zhou (Eds.), *Climate change 2021: The physical science basis. Contribution of Working Group I to the Sixth Assessment Report of the Intergovernmental Panel on Climate Change* (pp. 817–922). Cambridge University Press. https://doi.org/10.1017/9781009157896.008

Turner, A. J., Frankenberg, C., and Kort, E. A. (2019). Interpreting contemporary trends in atmospheric methane. *Proceedings of the National Academy of Sciences*, **116**(8), 2805–2813. https://doi.org/10.1073/pnas.1814297116

Ukhurebor, K. E., Aidonojie, P., Olayinka, A. S., and Nwankwo, W. (2024). Environmental influence of gas flaring: Perspective from the Niger Delta region of Nigeria. *Geofluids*, 2024, Article 1321022. https://doi.org/10.1155/2024/1321022

UNEP and CCAC. (2021). *Global Methane Assessment: Benefits and costs of mitigating methane emissions*. United Nations Environment Programme and Climate and Clean Air Coalition. Available at: https://www.unep.org/resources/report/global-methane-assessment-benefits-and-costs-mitigating-methane-emissions

Veefkind, J. P., Aben, I., McMullan, K., Förster, H., de Vries, J., Otter, G., Claas, J., Eskes, H. J., de Haan, J. F., Kleipool, Q., van Weele, M., Hasekamp, O., Hoogeveen, R., Landgraf, J., Snel, R., Tol, P., Ingmann, P., Voors, R., Kruizinga, B., ... Levelt, P. F. (2012). TROPOMI on the ESA Sentinel-5 Precursor: A GMES mission for global observations of the atmospheric composition for climate, air quality and ozone layer applications. *Remote Sensing of Environment*, **120**, 70–83. https://doi.org/10.1016/j.rse.2011.09.027

WMO. (2021). *WMO greenhouse gas bulletin: The state of greenhouse gases in the atmosphere based on global observations through 2020* (Bulletin No. 17). World Meteorological Organization. Available at: https://library.wmo.int/doc_num.php?explnum_id=10904

Yin, Y., Chevallier, F., Ciais, P., Broquet, G., Fortems-Cheiney, A., Pison, I., and Saunois, M. (2021). Decadal trends in global CO emissions as seen by MOPITT. *Atmospheric Chemistry and Physics*, **21**(16), 13053–13068. https://doi.org/10.5194/acp-21-13053-2021

Zhang, Y., Jacob, D. J., Lu, X., *et al*. (2021). Attribution of the accelerating increase in atmospheric methane during 2010–2018 by inverse analysis of GOSAT observations.

Atmospheric Chemistry and Physics, **21**(5), 3643–3666. https://doi.org/10.5194/acp-21-3643-2021

Zhu, L., Zhou, C., Yang, D., *et al*. (2025). Estimating methane emissions by integrating satellite regional emissions mapping and point-source observations: Case study in the Permian Basin. *Remote Sensing,* **17**(18), 3143. https://doi.org/10.3390/rs17183143